minerals

MDPI

Article

The Distribution of Rare Metals in the LCT Pegmatites from the Giraúl Field, Angola

Antonio Olimpio Gonçalves [1], Joan-Carles Melgarejo [2], Pura Alfonso [3,*], Sandra Amores [2], Andrés Paniagua [4], Andrés Buta Neto [1], Eduardo Alves Morais [1] and Antoni Camprubí [5]

1 Departamento de Geologia, Faculdade de Ciências, Universidade Agostinho Neto, Av. 4 de Fevreiro 71, Caixa Postal 815, Luanda 2131, Angola; tonygoncalves72@hotmail.com (A.O.G.); anbuneto@hotmail.com (A.B.N.); mlmorais@netangola.com (E.A.M.)

2 Departament de Mineralogia, Petrologia i Prospecció Geològica, Facultat de Ciències de la Terra, Universitat de Barcelona, Carrer de Martí i Franquès s/n, 08028 Barcelona, Spain; joan.carles.melgarejo.draper@ub.edu (J.-C.M.); sandra.amores.casals@gmail.com (S.A.)

3 Departament d'Enginyeria Minera, Industrial i TIC, Universitat Politècnica de Catalunya, Avinguda de les Bases de Manresa 61–73, 08242 Manresa, Spain

4 Departamento de Ciencias de la Tierra, Universidad de Zaragoza, Calle Pedro Cerbuna 12, 50009 Zaragoza, Spain; paniagua@unizar.es

5 Instituto de Geología, Universidad Nacional Autónoma de México, Ciudad Universitaria, 04510 Coyoacán, Mexico; camprubitaga@gmail.com

* Correspondence: maria.pura.alfonso@upc.edu; Tel.: +34-938777292

Received: 29 August 2019; Accepted: 23 September 2019; Published: 24 September 2019

Abstract: The Giraúl granitic pegmatite field in Angola is composed of five pegmatite types, the most evolved belong to the beryl-columbite, beryl-columbite-phosphate and spodumene types. Pegmatites are concentrically zoned with increased grain size toward a quartz core; the most evolved pegmatites have well-developed replacement units. These pegmatites are rich in Nb-Ta oxide minerals and the field has a moderate interest for critical elements such as Ta and Hf. Tourmaline, garnet and micas occur as accessory minerals. The abundance of Zr and Nb-Ta minerals increases with the evolution of the pegmatites, as well as the proportions of beryl and Li-rich minerals. The Ta/(Ta + Nb) ratio in Nb-Ta oxide minerals and the Hf/(Hf + Zr) ratio in zircon also increase with the evolution of the pegmatites and within each pegmatite body from border to inner zones, and especially in the late veins and subsolidus replacements. Textural patterns and occurrence of late veins with Ta-rich minerals suggest that Nb and especially Ta can be enriched in late hydrothermal fluids exsolved from the magma, along with Hf and other incompatible elements as Sn, U, Pb, Sb and Bi.

Keywords: pegmatites; columbite-group minerals; pyrochlore supergroup; niobium; tantalum; beryllium; hydrothermal; Angola

1. Introduction

Granitic pegmatites present a broad diversity of mineral species of great economic interest, and are an important source of rare metals, such as Li, Rb, Cs and Ta. In addition, they have been considered a potential source of other rare metals, such as Ga, Be, Sn, U, Nb, Hf, among others [1]. Pegmatites are, in addition, a source for high-quality industrial minerals (mainly feldspars, kaolinite, quartz, micas, and spodumene for ceramics) or gemstones such as topaz, tourmaline, aquamarine, spodumene, among others [2].

The study of Nb-Ta minerals is of great interest from both economic and scientific point of view. New technologies, especially those for the manufacture of electronic devices of small dimensions, have caused an increase in the need for tantalum [3,4]. The geochemical evolution of the Nb-Ta

minerals is quite characteristic in granites and pegmatite rocks and gives us information about their petrogenesis [5,6]. However, controversy persists regarding the mechanisms responsible for the concentration of Nb and Ta. The similar characteristics of the atoms of Nb and Ta cause both elements to have a similar geochemical behaviour: both are highly incompatible elements in magmatic systems. However, in highly evolved systems these elements follow different paths. Usually, the tendency followed in granitic pegmatites ranges from compositions rich in Nb and Fe to compositions rich in Ta and Mn [7]. However, anomalous behaviour of this trend can be produced by coeval crystallisation of other mineral phases that host some Nb and Ta, such as micas [8–11]. Therefore, a strong knowledge of the processes that generate the source rocks of these rare elements is necessary to understand the mechanisms of transport and accumulation of Nb-Ta oxides. Niobium and tantalum concentrate during the magmatic crystallisation by fractionation processes [12,13]. However, in the late processes of pegmatite evolution, such as those that form albitites, a Ta-enrichment is usually produced together with a high increase in the amount of Nb-Ta oxide minerals [11]. This enrichment has been explained considering strictly magmatic processes by extreme fractionation during crystallisation process [2,9,14–17]. However, late hydrothermal fluids exsolved during the late stages of magmatic crystallisation were also considered as responsible for the Ta-richest mineralisation in pegmatites and rare-metal granites [18–20]. Textural evidences play an important role to the validation of these hypotheses [20,21].

The Giraúl pegmatite field (Angola) outcrops in a desert area, and the outcrops are exceptional. It is an excellent place to study the relation of pegmatites with granites and host rocks, their internal structure and the mineral distribution. In addition, a mining company explored some mineralised pegmatites for muscovite and beryl during the Portuguese colonial times, up to the 1980s but wars prevented any operation during decades. In this contribution we aim to describe the characteristics of the Giraúl pegmatites in Angola with special emphasis on their structure, distribution of critical minerals, mineralogy and mineral chemistry of Nb-Ta minerals in order to discuss about the processes that control the enrichment in critical elements.

2. Geology

2.1. Regional Geology

The outermost pegmatite outcrops occur about 15 km East of Namibe, a town located 600 km south of Luanda and the pegmatite field outcrops in a belt 20 × 8 km trending WNW-ESE in the Giraúl desert. The Giraúl pegmatite field is included in the Angola shield, in the SW part of Angola, near the fault contact with the Perioceanic Depression, which is filled with sedimentary rocks of Lower Cretaceous age and Quaternary sediments. The Giraúl pegmatites (Figure 1) are mainly hosted in an Upper Archean greenstone belt comprising layers of muscovite-biotite schists interbedded with thick units of volcanic rocks. The ensemble was been affected by a regional metamorphism to the amphibolite facies and deformed by two Precambrian stages of folding. The main direction of folds and the main cleavage are NW-SE. These materials were intruded by small stocks of Late Eburnean pyroxenites to gabbro-norites, followed by a sequence of granitic rocks ranging from diorites to biotite-muscovite leucogranites and, finally, the pegmatites. Granitic outcrops were emplaced in the axis of the folds and pegmatites along the regional cleavage. Some of the pegmatites intrude these granites or surround them. The pegmatite field is cut by NE-SW and NW-SE strike-slip fault systems, which distort the zoning and favour the emplacement of Cretaceous diabase dykes. Both fracturing and late magmatism are associated with the opening of the South Atlantic. All these rocks are affected by erosion of Lower Cretaceous age and unconformably covered by Cretaceous conglomerates, sandstones and, locally, basic volcanic rocks [22]. The faults have a critical importance in the structure of the pegmatite field: they compartmentalize it into blocks. Consequently, they distort the original zonation of the field, by bringing into contact highly evolved and less evolved areas. Therefore, this distribution must be taken into account when thinking about a strategy to explore rare elements in a zoned pegmatite field.

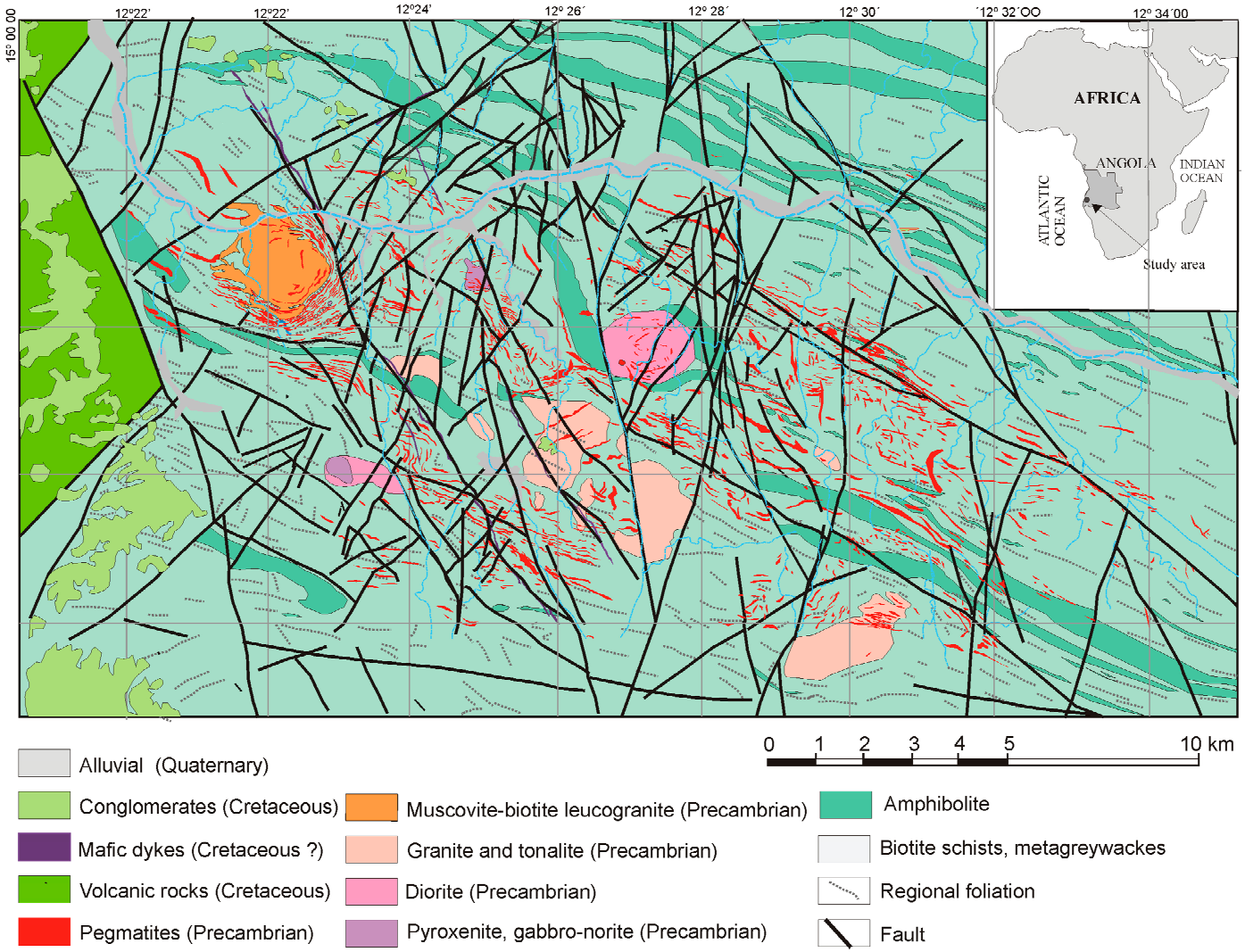

Figure 1. Geological map of the Giraúl pegmatite field.

About 600 pegmatite bodies outcrop in the pegmatite field. Most of them are lens-shaped, although some of them have a droplet shape; they can be from 5 m up to 1 km in length. The pegmatite dykes are arranged WNW-ESE following the regional foliation. The contacts between pegmatites and the host rocks, including most of the igneous rocks, are generally sharp. However, the contacts between pegmatites and the hosting leucogranite are gradational, thus indicating that these pegmatites may well be produced by fractionation of the most evolved granite magmas.

2.2. Pegmatite Types

The Giraúl pegmatite field is composed of a wide variety of pegmatites, which can be differentiated each other using structure and mineralogy. Along with field criteria, we adopt the following the classification of [23,24], into five types of pegmatites in the Giraúl pegmatite field, all of them corresponding to the lithium-cesium-tantalum LCT family (Figure 2).

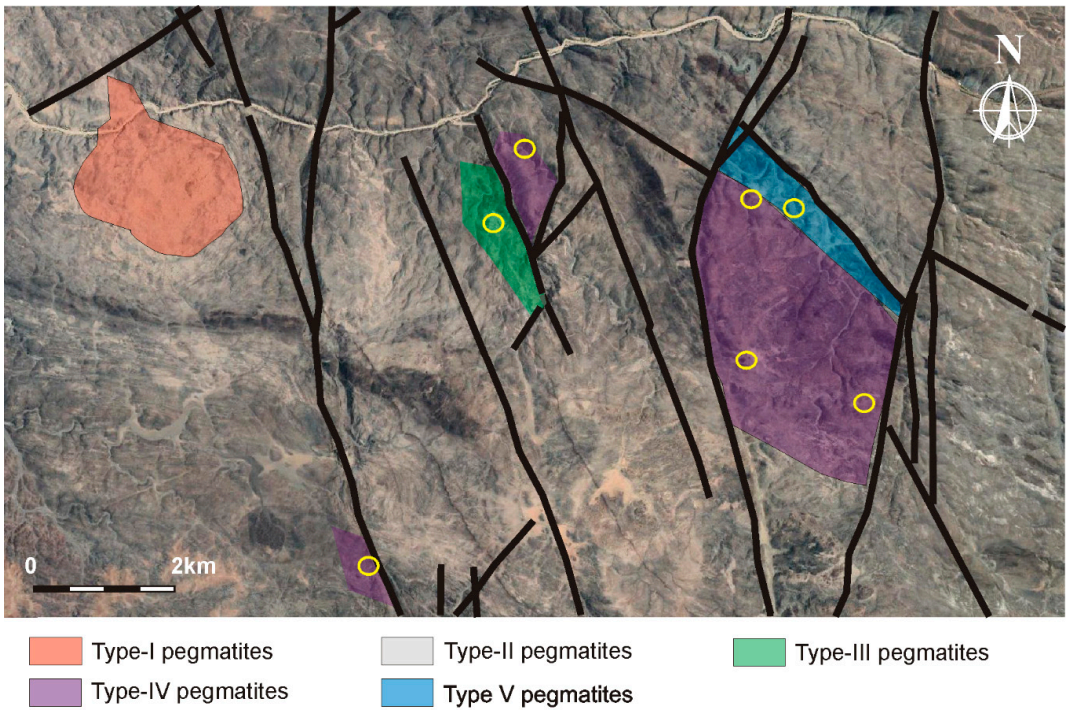

Figure 2. Google Earth satellite image showing the distribution of the Giraúl pegmatite types. Type-II pegmatites occur over all the area. Circles indicate outcrops of mined pegmatites.

Type I are microcline-bearing intrabatholitic pegmatites; type II are microcline-bearing peribatholitic pegmatites; type III are beryl-columbite pegmatites; type IV are beryl-columbite-phosphate pegmatites, and type V are petalite-bearing pegmatites. Figure 3 shows some field images of these types of pegmatites.

2.2.1. Type-I Pegmatites

Type-I pegmatites are lensoidal or tabular bodies hosted in leucogranite with a single internal structure and mineralogy (Figure 4). They do not have border zone, and the contact with the host leucogranite is gradational. The first intermediate zone resembles a coarse-grained granite, and a second intermediate zone is constituted by blocky K-feldspar intergrown with quartz. Tourmaline and garnet are abundant accessory minerals. The most abundant mica is muscovite, but biotite can also occur and usually it is replaced by epitactic crystals of muscovite. Other accessory minerals are zircon, fluorapatite, monazite, xenotime and uraninite. Euhedral crystals of green beryl are common in the

contact with the quartz core, which can be of the rose variety. These pegmatites are almost devoid of minerals with rare elements, except for zircon.

Figure 3. Outcrops from the Giraúl pegmatites. (**a**) type-II pegmatites, (**b**) large type II pegmatite, (**c**) subhorizontal dykes of type-III pegmatites, (**d**) general view of a type III pegmatite, (**e**) Quartz-muscovite vein of the type-III pegmatite, (**f**) general view of a type-V pegmatite.

2.2.2. Type-II Pegmatites

Type-II, or beryl-columbite pegmatites, are the most abundant in the Giraúl field; more than 400 bodies belonging to this category are hosted in the metamorphic Precambrian rocks and in intermediate to basic plutonic rocks. They are distributed throughout the field, although the highest density of dykes occurs as concentric rings surrounding the leucogranite stocks at the NW of the area. They have variable dimensions, usually more than 200 m long and several tens of meters wide (Figure 2). The contact between pegmatites and host rocks is sharp at the outcrop scale, although in detail

metasomatism can be present in the metamorphic host rocks, typically consisting of tourmalinisation, biotitisation and muscovitisation.

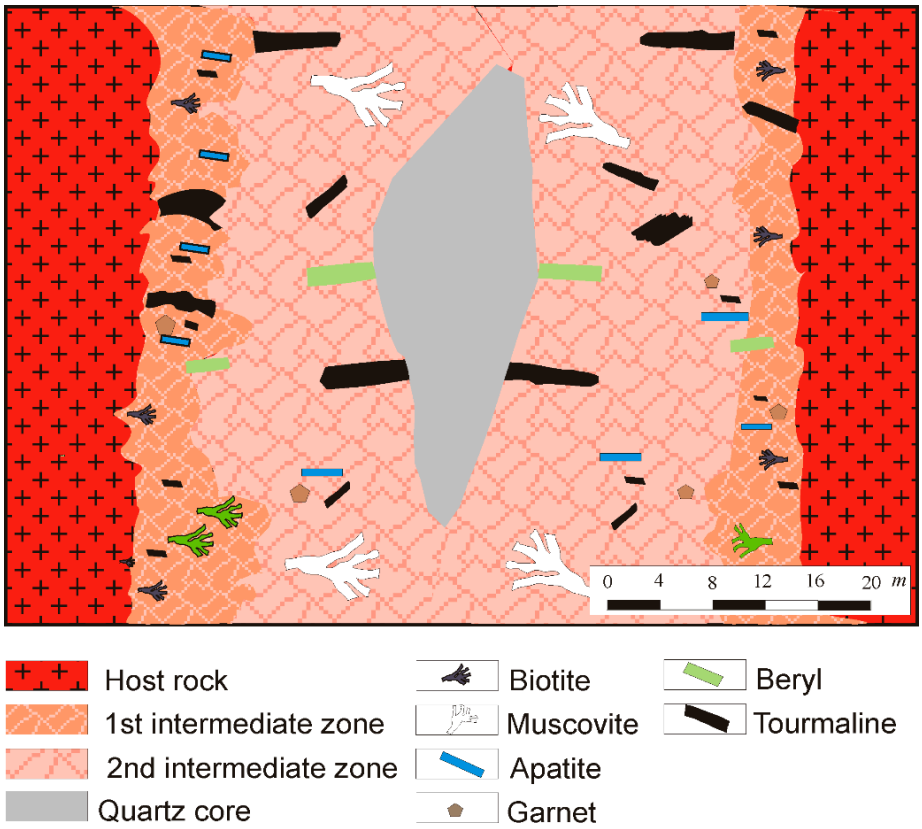

Figure 4. Conceptual scheme (not to scale) with the various pegmatite units in type-I pegmatites, showing the distribution of the most significant minerals.

The structure of type-II pegmatites includes five concentric zones: border, wall, first intermediate, second intermediate and quartz core (Figure 5). The five outermost zones are made up of graphic intergrowths of quartz and microcline, with minor albite, skeletal micas (muscovite and biotite) and apatite. Black tourmaline and garnet occur in minor amounts, and beryl is rare and only occurs in the second intermediate zone in contact with the core. These pegmatites are also poor in minerals of rare elements, with the exception of some scarce crystals of the columbite-group minerals (CGM) and zircon. The processes of metasomatic replacement of the primary minerals are almost nil, except in some slightly more evolved pegmatites of the group, where fine albite veins appear and replacement of K-feldspar by albite occurs at the microscopic scale.

2.2.3. Type-III Pegmatites

Type-III pegmatites occur in a distal position related to the leucogranite body, mainly following fractures in the hosting ultramafic rocks. Muscovite and tourmaline appear in the exocontact. Their structure (Figure 6) is similar to type II-pegmatites, but their mineralogy is more complex. Thus, for first time, significant amounts of CGM appear in the field, as well as other minerals of Nb-Ta and rare elements. Other common accessory minerals are blue apatite, beryl, zircon and yellowish muscovite. In addition to the five concentric zones, a third intermediate zone can be distinguished in these pegmatites. This zone has similar composition than the other intermediate zones but a larger grain size. Albitisation is not generalised but it is more abundant than in type-II pegmatites. Thin albite veins crosscut the intermediate zones.

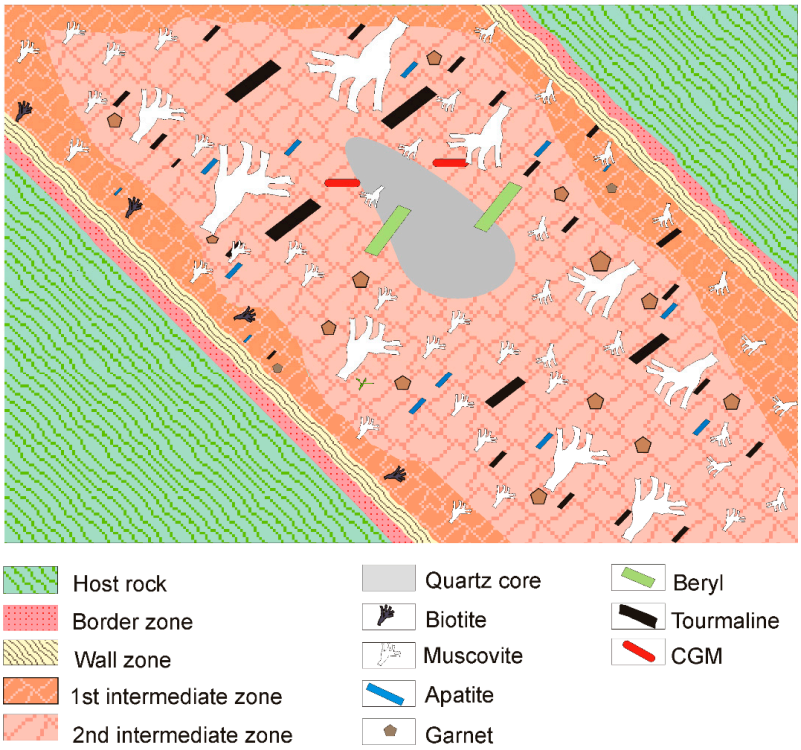

Figure 5. Conceptual scheme (not to scale) showing the pegmatite units in type-II pegmatites and the distribution of the most significant minerals.

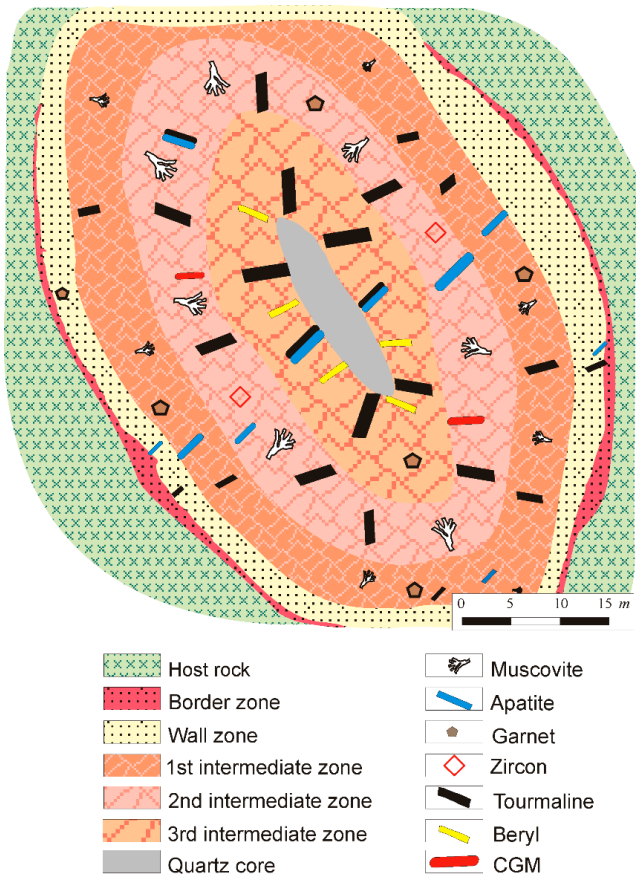

Figure 6. Conceptual scheme (not to scale) of the various pegmatite units in type-III pegmatites and distribution of the most significant minerals.

2.2.4. Type-IV Pegmatites

Type IV, or beryl-columbite-phosphate granitic pegmatites are evolved and rare-element-rich. They are hosted by amphibolites and diorites. Small pegmatites can show a simple structure; however, in most cases, the structure consists of the same units described in type-III pegmatites with the addition of well-developed advanced subsolidus replacement phenomena (Figure 7). On the other hand, a new characteristic in type-IV pegmatites is the existence of late veins cutting all the zoned units of the pegmatite but never crossing the contact with the host rock. These veins are from 1 mm to several tens of cm wide. Two types of veins are distinguished: the albite veins, which are associated with wide spread hydrothermally albitized areas and quartz-muscovite veins, formed later than the albitites. Hydrothermal alteration phenomena in the exocontact are strong in most of these pegmatites: holmquistite (Li amphibole) is formed in cases of pegmatite emplacement in amphibolites; tourmaline and muscovite are produced in case of emplacement in schists or granitic rocks.

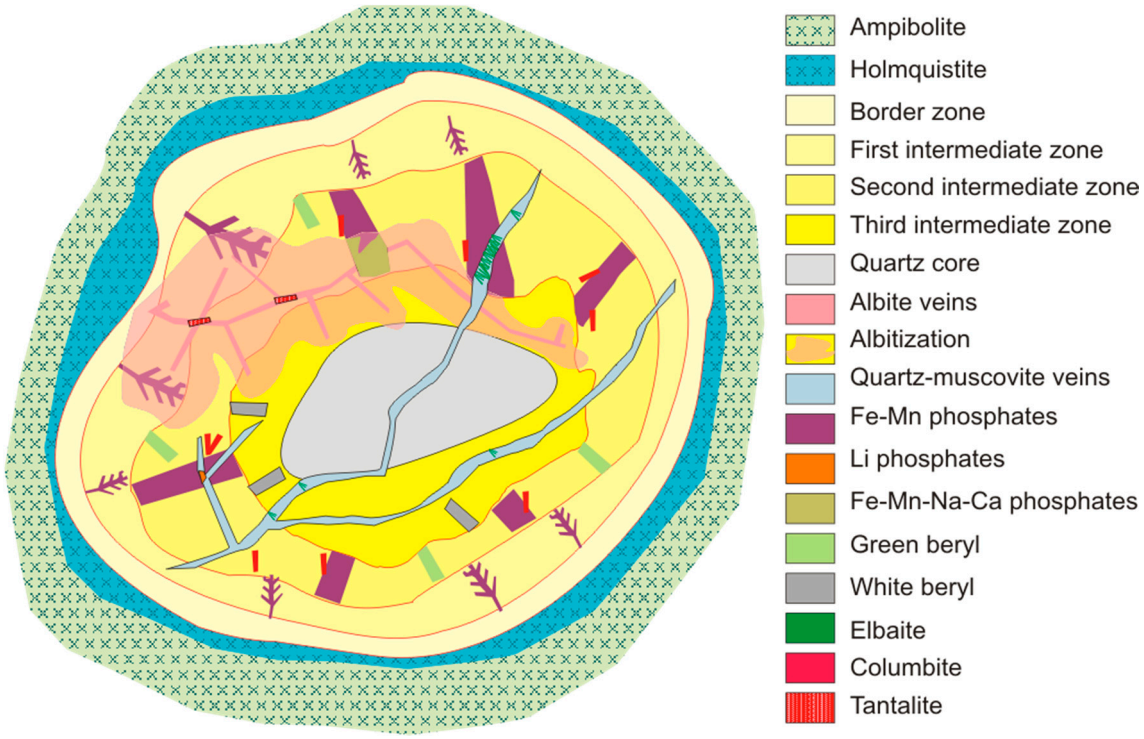

Figure 7. Conceptual scheme (not to scale) of the various pegmatite units in type-IV pegmatites and distribution of the most significant minerals.

They are also composed of quartz and microcline, along with large amounts of muscovite and moderate contents of garnet, tourmaline, Li-rich phosphates, beryl, cassiterite and a significant amount of Nb-Ta minerals. The border zone is coarse grained and consists of quartz, K-feldspar, oligoclase, muscovite, tourmaline, almandine and blue apatite. The first intermediate zone (coarse grained) mainly consists of reddish K-feldspar, quartz, albite, muscovite, green beryl and schorl; it contains skeletal crystals of phosphates (triphylite, ferrisicklerite, heterosite), and small amounts of Nb-rich members of the columbite-group minerals (CGM). The second intermediate zone contains similar minerals, but the phosphates tend to develop euhedral crystals up to several meters in length. Green beryl and CGM are also very abundant in these zones. The third intermediate zone is mainly made up of blocky white K-feldspar and white beryl, with lesser amounts of muscovite. Finally, some late veins, filled with quartz, albite, muscovite, tantalite, elbaite and montebrasite, crosscut all the previously mentioned units, producing the replacement of these. No quartz cores have been found so far.

2.2.5. Type-V Pegmatites

Type V, or petalite-bearing pegmatites, are the most evolved in the Giraúl field, at present, only one pegmatite of this type has been identified. This pegmatite intrudes in a very distal position in relation to the leucogranite stock and is located in schists of intermediate metamorphic grade (Figures 1 and 2). It is a 100 m-long drop-like body that crosscuts the foliation of the host rocks. This pegmatite has abundant Li-rich silicates and phosphates, and is of interest as a source of rare elements. It does not have a well-defined zonal structure (Figure 8). The of the earlier zones is similar to that mentioned for the less evolved pegmatites. However, in a late blocky unit is a Li-rich paragenesis, comprising spodumene, petalite, lepidolite, pink or green elbaite and amblygonite. Cassiterite and tantalite also are abundant.

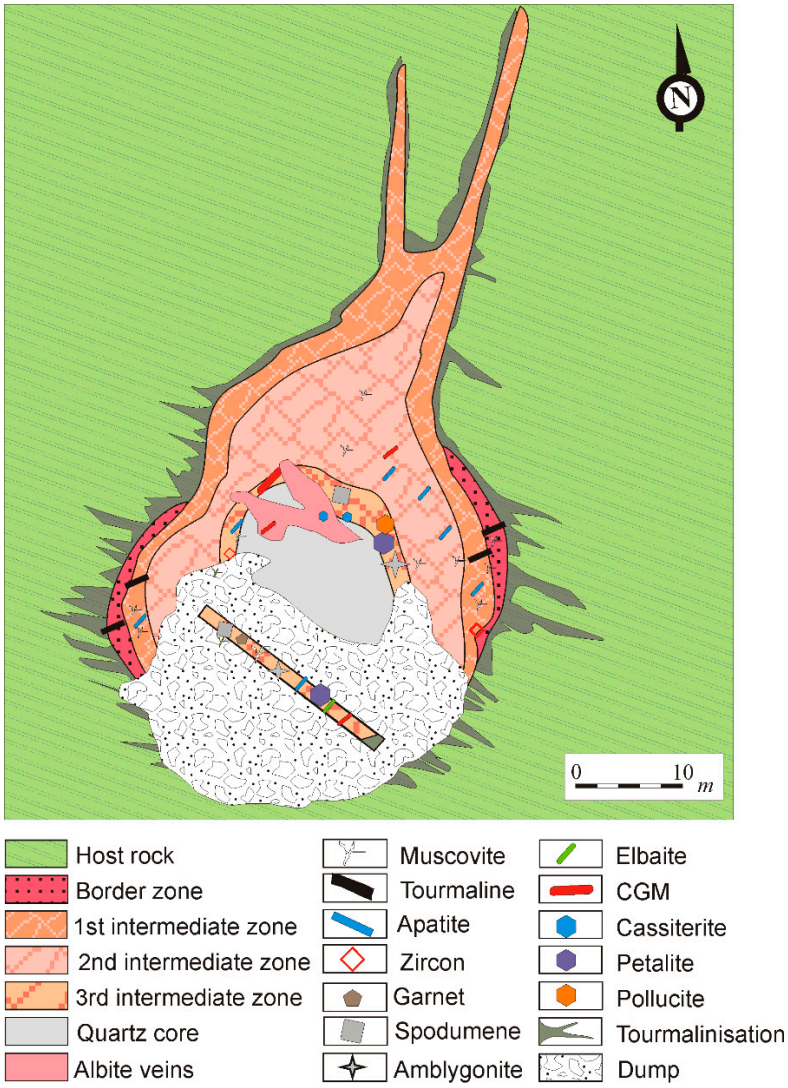

Figure 8. Conceptual scheme (not to scale) of the various pegmatite units in the type-V pegmatite and distribution of the most significant minerals.

3. Analytical Methods

Petrographic and mineralogical characterisations were carried out by X-ray powder diffraction (XRD), optical microscopy and scanning electron microscopy. The XRD spectra were measured on powdered samples in a Bragg-Brentano PANAnalytical X'Pert Diffractometer (graphite monochromator, automatic gap, Kα-radiation of Cu at λ = 1.54061 Å, powered at 45 kV–40 mA, scanning range 4–100° with a 0.017° 2θ step scan and a 50 s measuring time. Identification and Rietveld

semiquantitative evaluation of phases was made on PANanalytical X'Pert HighScore software (Version 2.0.1, PANanalytical, Almelo, The Netherlands).

The compositional zoning of Nb-Ta minerals was examined by scanning electron microscopy with energy-dispersive X-ray spectroscopy (SEM-EDS) used in the back-scattered electron mode (BSE). The SEM-EDS equipment was an ESEM Quanta 200 FEI, an XTE 325/D8395 (Thermo Fisher Scientific, Waltham, MA, USA) equipped with an INCA Energy 250 EDS microanalysis system) was used. Mineral chemistry was obtained using electron-microprobe analyses (EMPA) carried out with a CAMECA SX-50 (Gennevilliers Cedex—France) located at the Scientific and Technological Centers of the University of Barcelona. Analyses were conducted at an accelerating voltage of 20 kV, an electron beam current of 20 nA, and a beam diameter of 2 μm. Standards used were: $Li_2Nb_2O_6$ (Nb, Lα), $Li_2Ta_2O_6$ (Ta, Lα), W (W, Kα), rutile (Ti, Kα), cassiterite (Sn, Kα), YAG (Y, Lα), U (U, Mα), ThO_2 (Th, Mα), Sb_6 (Sb, Mα), Bi_6 (Bi, Mα), Pb (Pb, Mα), Sc (Sc, Kα), periclase (Mg, Kα), hematite (Fe, Kα), rhodonite (Mn, Kα), wollastonite (Ca, Kα), albite (Na, Kα), Sr (Sr, Kα), baryte (Ba, Lα), orthoclase (K, Kα). Detection limits for trace elements were 0.01 wt.%. The structural formulae of the CGM were calculated on the basis of 24 atoms of oxygen and 12 cations per unit cell (apfu) for CGM. The number of cations was fixed by a method of charge balance by conversion of part of Fe^{2+} to Fe^{3+} as proposed by Ercit et al. [7]. The structural formula of tapiolite and cassiterite were calculated on the basis of 6 and 4 atoms of oxygen per formula unit, respectively. The structural formula of pyrochlore-supergroup minerals was calculated on the basis of a fully occupied B site (Nb + Ta + W + Ti = 2 apfu), and OH^- was calculated by charge-balance to an anion total of 7 [25].

4. Mineralogy of the Giraúl Pegmatites

4.1. Mineralogical Composition and Textural Patterns

There are considerable variations in the mineralogical composition of the Giraúl pegmatites throughout the field, from type-I to type-V pegmatites. The variation in the mineral composition affects both the major and accessory minerals, in particular, the rare-element-rich minerals.

Plagioclase from the first intermediate zone of type-I pegmatites has an intermediate composition, which is evidence of a low degree of evolution. The composition of this plagioclase resembles that present in the host leucogranites, which demonstrate the genetic relationship of the pegmatites with their host granites. However, in the second intermediate zone, the composition of the plagioclase attains the compositional domain of albite, and this, for the rest of the pegmatite field. The mineral composition of the pegmatite is very simple in the two intermediate units, with quartz, albite and microcline (Figure 9a).

In addition, an important difference of type-I pegmatites in relation to the others is the presence of rose quartz in the pegmatite core (Figure 9b). This core has not a homogenous colour. The pink colouring of quartz has been attributed to the presence of nano-sized fibers of dumortierite [26–28]. In pegmatites this borosilicate usually appears in grains of less than 1 μm.

Accessory minerals in type-II pegmatites include small amounts of CGM, scarce biotite, and widespread green apatite crystals. The presence of biotite, although limited to less evolved type-II pegmatites located closest to leucogranites, is very significant, since this mineral is absent in the parental leucogranites and, in type-I pegmatites, where muscovite is found exclusively. This indicates that Fe and Mg necessary to form this mineral come from the contamination of the pegmatite by the host rocks. This biotite is unstable and often it is replaced by muscovite. The other novel aspect, the appearance of Nb-Ta minerals respect to more primitive pegmatites, occurs to a relatively insignificant extent, as these minerals are confined to the late stages of crystallisation, and are found in extremely low proportions.

In type-III pegmatites, abundant CGM appear, as well as late replacements of them by pyrochlore-supergroup minerals.

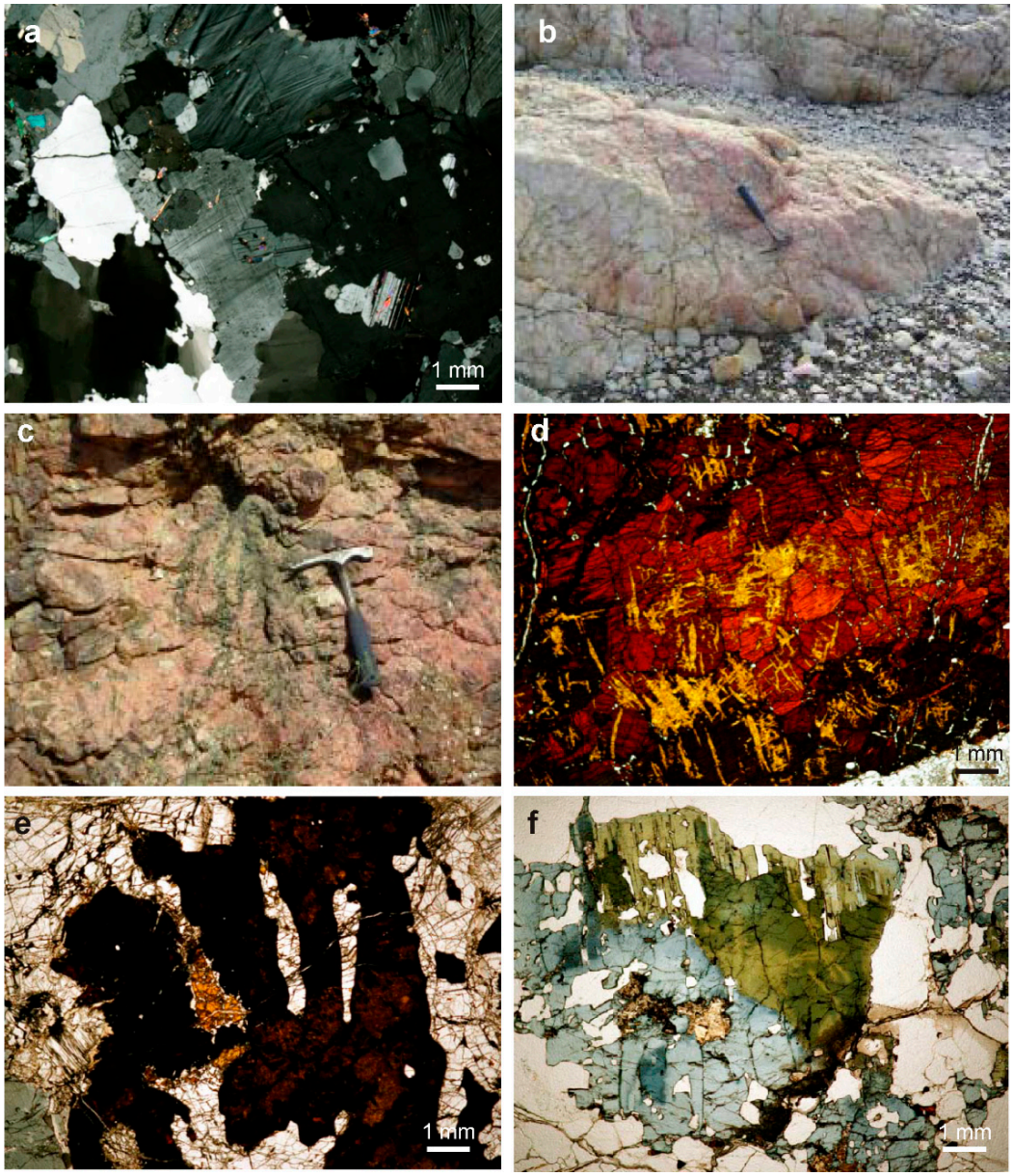

Figure 9. Textural patterns in pegmatites: (**a**) Microscope image of an intergrowth of microcline and quartz from the First intermediate zone of type-I pegmatites. (**b**) Large quartz core in type-I pegmatite, in which some areas with pink quartz are distinguished in a predominantly white core. (**c**) Skeletal crystals (or graphic intergrowths) of altered triphylite (dark) with reddish K-feldspar, in the first intermediate zone of a type-IV pegmatite. (**d**) Replacement of ferrisicklerite (orange) by heterosite (red); the whole is cut by alluaudite (greenish yellow). Thin section, PPL. (**e**) Skeletal intergrowths of triphylite altered to secondary phosphates; the interstitial material is albite. Thin section, PPL. (**f**) Skeletal crystals of tourmaline, strongly zoned, in graphic intergrowths with quartz, in the first intermediate zone of a type-IV pegmatite. Thin section, PPL.

Type-IV pegmatites have higher contents of minerals of critical elements: primary lithium phosphates (Figure 9c), elbaite, cassiterite and Ta- and Mn-rich members of the CGM. The most characteristic aspect of these pegmatites is the appearance of large crystals of phosphates, they are essential minerals in the intermediate zones, particularly in the second intermediate zone. These minerals occur as skeletal crystals in the first units, and form more regular crystals toward the innermost units. The presence of skeletal phosphates (Figure 9d) is common in pegmatites worldwide [29–31].

Not only phosphates have this type of crystallisation but, in general, all the minerals of the intermediate zones of all the pegmatites, being especially shown in tourmaline, muscovite, garnet and feldspars (Figure 9f) and this texture has been attributed to rapid growth in undercooled melts [32]. The primary phosphate phases identified are montebrasite and ferrisicklerite, which are replaced by heterosite, suggesting that primary triphylite may have existed. Remnants of this primary triphylite have been found, although they are completely replaced by secondary phosphates. Therefore, these minerals are part of the known sequence initially described by Quensel [33] and Mason [34] in the pegmatites of Varuträsk (Sweden), and later located in most of the pegmatite fields containing phosphates, such as Tsaobismund in Namibia [35], Albera in the French Pyrenees [36], and in Jocão, Minas Gerais, Brazil [37].

An important aspect in these pegmatites is change of coloration of K-feldspar, from the first intermediate zones (reddish owing to minute hematite inclusions) to the third ones (white). Therefore, an important aspect of these pegmatites is the high proportion of Fe in the first intermediate zones, which drastically decrease in the third. Possibly this is due to the crystallisation of large amounts of Fe phosphates in the early units.

Another remarkable aspect of these pegmatites is the appearance of giant crystals of white beryl in the third intermediate zones, at that the stage at which there is no availability of Fe. Finally, Ta-poor CGM occur in the intermediate zones the crystallisation, which completes the typical association of beryl-columbite-phosphate.

The most significant aspect of these pegmatites is the appearance of albite veins and veins of quartz-muscovite-elbaite. Intensive phenomena of albitisation of the primary K-feldspar of the intermediate zones are produced in the vicinity of these veins; K-feldspar can often be completely replaced. In addition, the hydrothermal fluids associated with this episode produce the substitution of primary phosphates by alkali-rich phosphates of the alluaudite group. These veins are strongly enriched in fine-grained crystals of tantalite-(Fe) and tantalite-(Mn).

The quartz-muscovite-elbaite veins are not very common, but they are significant as they indicate that there is, even in the late stages of crystallisation, a hydrothermal phase that carries Li. Elbaite formed by the replacement of primary lithium phosphates, suggesting that possibly Li is remobilised during the replacement of the primary phosphates. In these veins, a high activity of fluorine is registered, as suggests the presence of minerals rich in this element, such as amblygonite.

Type-V pegmatites are the most evolved in the field. Although important amounts of spodumene associated with amblygonite-montebrasite appear in the third intermediate zone of these pegmatites, the rest of the pegmatite is very similar to the type-III pegmatites, as it does not contain primary phosphates in the first intermediate zone, and lithium seems to have concentrated in the third intermediate zone. The large spodumene crystals are primary, but a second generation has been produced by the replacement of petalite, where a symplectitic spodumene-quartz intergrowth (SQU) is formed. This is formed by a typically retrograde reaction [38], and is common to many pegmatite fields, such as at Lake Khibara, in Natal, South Africa [39], and Tanco in Manitoba, Canada [40].

In the late veins of these pegmatites, the micas show compositional zoning, evolving toward their rim to mica rich in Li, Rb and Cs. In the final stages, nanpingite replaces muscovite. This mineral is very rare and is considered an indicator of fractionation [41,42]. In the pegmatites of Oktyabrskaya, in Transbaikalia (Russia), nanpingite appears in melt-fluid inclusions, which could represent a transition from magmatic to hydrothermal state [43]. At Giraúl the formation of nanpingite is attributed to the partition of Cs to the late fluid phase. In addition, these late veins contain most of the elbaitic tourmaline, as well as cassiterite, Ta-rich CGM, and gahnite.

4.1.1. Textural Patterns of Zircon

Zircon crystals of type-I pegmatites are fine grained, in the order of 70 μm, and rare. In type-II pegmatites, zircon is also rare and, in thin section, presents dirty, greyish colorations due to metamictisation. These are idiomorphic crystals of prismatic habit, with dipyramidal faces. Zircon has

a concentric zoning, and is almost invariably isotropic because of metamictisation, especially in the core of the crystal.

In type-III pegmatites, also zircon can occur in the wall and in the three intermediate zones as fine-grained euhedral crystals, strongly metamict (Figure 10a–c).

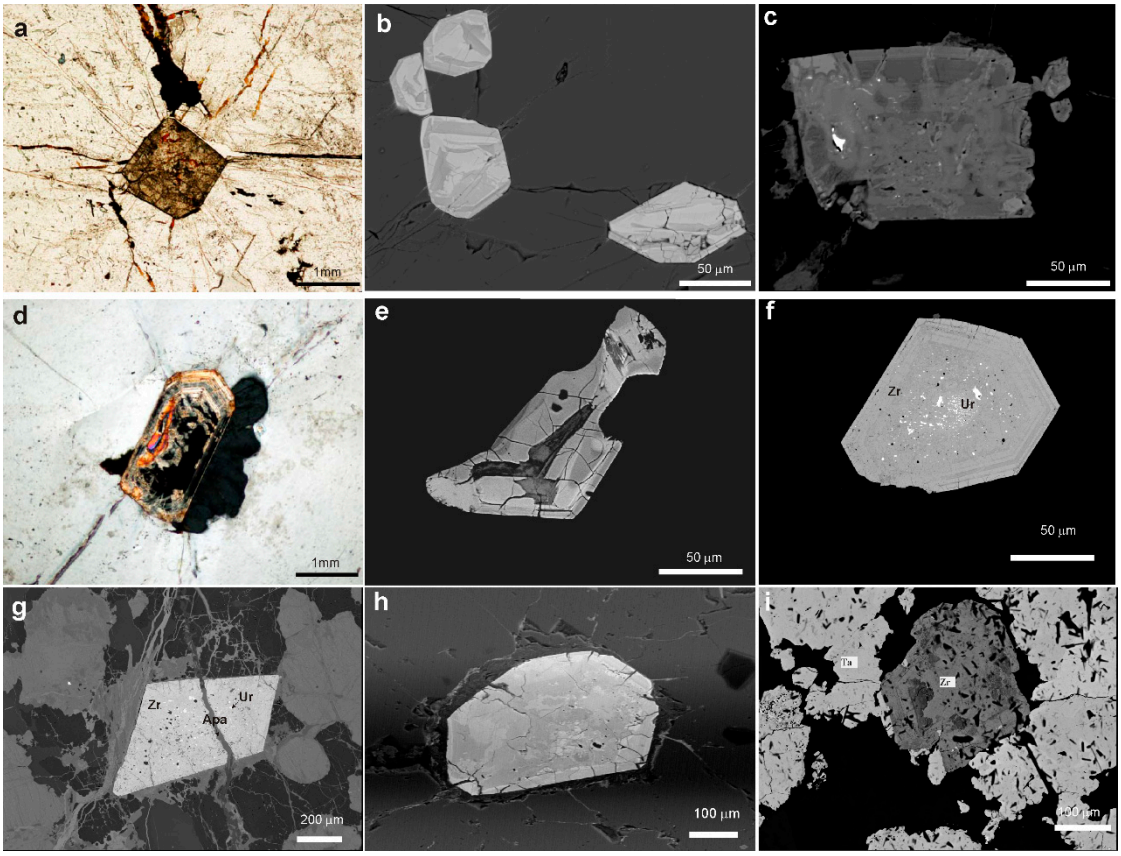

Figure 10. Textural patterns of zircon in type-III pegmatites. (**a**) Transmitted optical microscope image of zircon crystal included in plagioclase showing radial fractures produced during metamictisation, PPL. (**b**) Euhedral zoned zircon crystals. SEM image, BSE mode. (**c**) zircon crystal with convoluted zoning. SEM image, BSE mode. (**d**–**g**) Textural patterns of zircon in type-IV pegmatites. (**d**) Transmitted optical microscope image of a zoned zircon crystal with metamict core, XPL. (**e**) Zoned zircon crystal with high content in Hf (bright areas) and poorer (dark) areas. SEM image, BSE mode. (**f**) Zircon crystal with small inclusions of uraninite, cut by apatite vein in an association with triphylite, heterosite and quartz. SEM image, BSE mode. (**g**–**i**) Textural patterns of zoned zircon from type-IV pegmatites. SEM images, BSE mode.

Zircon crystals are very unevenly distributed in type-IV pegmatites; they are fine-grained and are moderately zoned; on the other hand, they are usually metamict (Figure 10d–g). They are relatively common in the second intermediate zone of type-IV pegmatites. These are idiomorphic crystals with a short prismatic habit, 1–2 mm long, composed of a prism and a tetragonal dipyramid. They have a concentric zonation and are very altered, with isotropic metamict areas. In most cases, zircon occurs as inclusions in other minerals, or in quartz veins that cut primary phosphates.

Zircon is a common mineral in the type-V pegmatite, although generally it has very small grain-size; the larger crystals reach about 100 µm, although they are generally smaller than 1 µm, only distinguishable by their radioactive aureoles where they are included in phyllosilicates. Zircon crystals are euhedral with prism and bipyramid forms, commonly corroded. They are included in other minerals, such as columbite-tantalite. They present a concentric zoning, although distorted by

alteration, since this mineral is usually metamict (Figure 10h,i), which removes all possibilities to use in dating.

4.1.2. Textural Patterns of the Nb-Ta Oxide Minerals

The variety and abundance of Nb-Ta rich oxide minerals increase from type-II to type-V pegmatites. In type II pegmatites, Nb-Ta oxides are very rare and limited to CGM located in the second intermediate zone, especially in contact with the quartz core. They form scarce unzoned hemihedral crystals of less than 50 μm in size, and do not seem zoned.

In type-III pegmatites, most of Nb-Ta oxides are CGM, but there are also some minerals of the pyrochlore supergroup, tapiolite, stibiocolumbite and stibiotantalite groups. The CGM can appear with two different aspects (Figure 11a,b): (a) euhedral crystals up to 1 mm in length that have a convoluted zoning, with Ta- and Nb-rich areas, and (b) euhedral crystals, up to 0.5 cm in size, where no zonation is observed (Figure 11c). Pyrochlore supergroup minerals occur in fine veinlets within the non-zoned columbite-(Fe) crystals (Figure 11c,d).

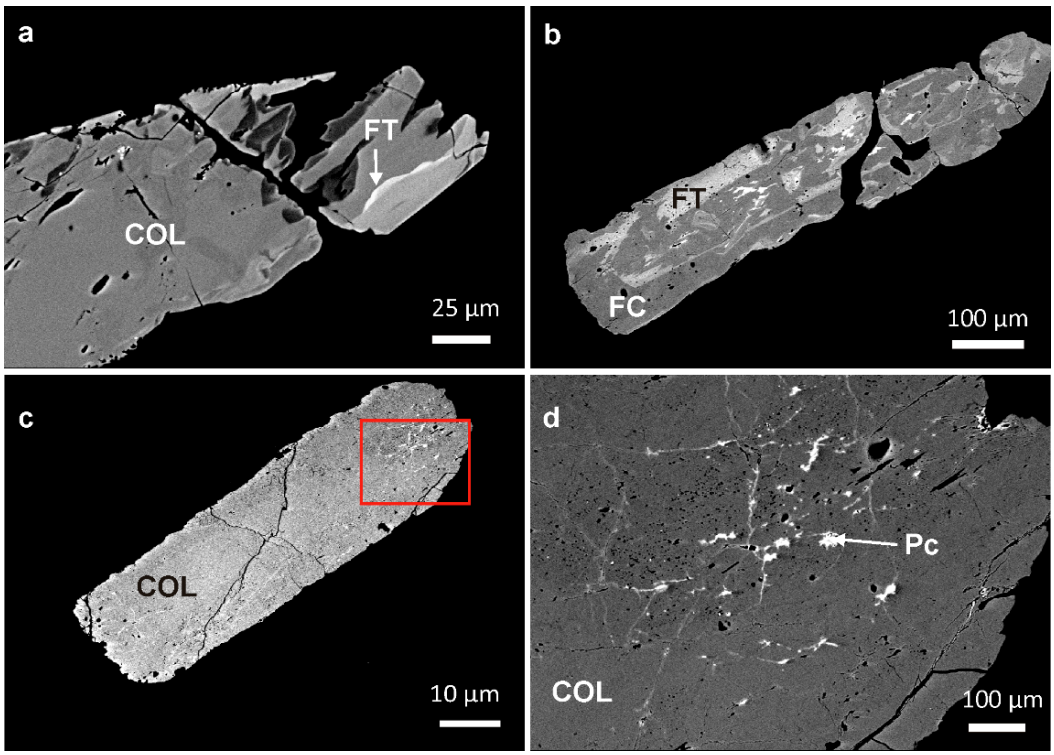

Figure 11. Textural patterns of CGM from type III pegmatites. (**a**,**b**) Columbite and tantalite with convoluted zoning. (**c**) Unzoned columbite crystal with late pyrochlore replacements. (**d**) detail of the area from image c with replacements by pyrochlore-supergroup minerals (Pc). Col, FC, columbite-(Fe); FT, tantalite-(Fe).

Beryl-columbite-phosphate pegmatites (type IV) are rich in Nb-Ta oxides. In all of the studied pegmatite bodies, these minerals belong mainly to the columbite group, with minor amounts of rutile, tapiolite and members of the stibiotantalite and pyrochlore supergroup. The Nb-Ta minerals generally are less than 200 μm across, but they reach sizes up to 5 cm in the second intermediate zone. Crystals of the CGM present slight compositional zoning or a moderately marked convoluted zoning. In the first intermediate zone, these minerals form euhedral homogeneous crystals or with a weak zoning, whereas in the second intermediate zone, crystals with a strongly convoluted zoning can occur (Figure 12). Pyrochlore-supergroup minerals replace CGM crystals, generally in veinlets, although rare euhedral crystals may occur (Figure 12i).

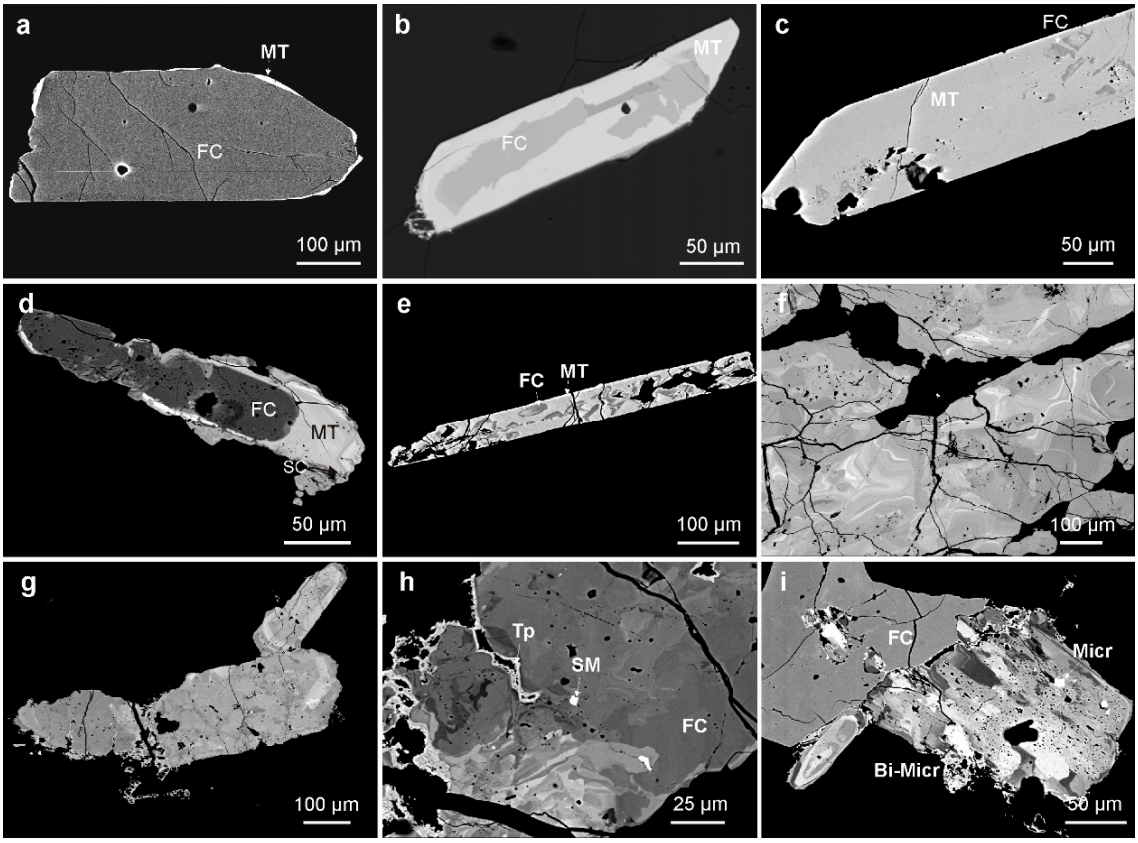

Figure 12. Textural patterns of Nb-Ta minerals from type-IV pegmatites, SEM images, mode BSE, (**a**) columbite-(Fe) crystal (FC) with a narrow tantalite-(Mn) rim (MT). (**b**) columbite-(Fe) crystal (FC) replaced by tantalite-(Mn) (MT), (**c**) tantalite-(Mn) crystal (MT) with minor columbite-(Fe) (FC) relict areas. (**d**) columbite-(Fe) (FC) partly rimmed by tantalite-(Mn) (MT) with a small grain of stibiocolumbite (SC), (**e**) columbite-(Fe) crystals with convoluted complex zoning, (**f**) detail of the above columbite crystal with convoluted zoning, with bands richer in Ta (lighter) and in Nb (darker). (**g**) columbite crystals with patchy complex zoning and replacements, (**h**) detail of image g, where replacements of patchy zoned columbite-(Fe) (FC) by stibiomicrolite (SM) and tapiolite (TP) in veinlets are more visible, (**i**) columbite-(Fe) crystal (FC) replaced by microlite (Micr) and Bi-rich microlite (Bi-Micr).

In the spodumene-type pegmatite (type V), the Nb-Ta oxides are found in the first, second and third intermediate zones. They are mainly formed by minerals of the CGM and pyrochlore supergroup. Stibiocolumbite and stibiotantalite, although present, are scarce. The CGM are abundant in the third intermediate zone, where they form euhedral tabular crystals 2–5 cm in size. As in the type-IV pegmatites, these crystals present a complex patchy zoning (Figure 13a,b), with abundant complex replacements by late fluids rich in Ta. On the other hand, they are fractured and replaced by generations of other Nb-Ta minerals and cassiterite (Figure 13c,d). Tantalite is abundant in the albite veins unit as euhedral crystals 1–2 mm in size.

The petalite-bearing pegmatite (V) is rich in a wide variety of the pyrochlore-supergroup minerals. These minerals appear in the second and, mainly, in the third intermediate zones. Microlite is a rare mineral in this pegmatite, having been identified only as a product of late replacement of the CGM, in which it fills small veinlets of a few µm wide (Figure 13), where it is associated with other Ta-poor minerals. Microlite occurs here usually as anhedral grains, with a round appearance, although occasionally euhedral crystals can be developed.

Finally, tapiolite occurs in the most evolved pegmatites filling veinlets or pore space in all the minerals of the pegmatite (Figure 14a,b), although it is more common replacing CGM crystals in veinlets or rimming them (Figure 14c,d), in some cases along with minerals of the pyrochlore supergroup.

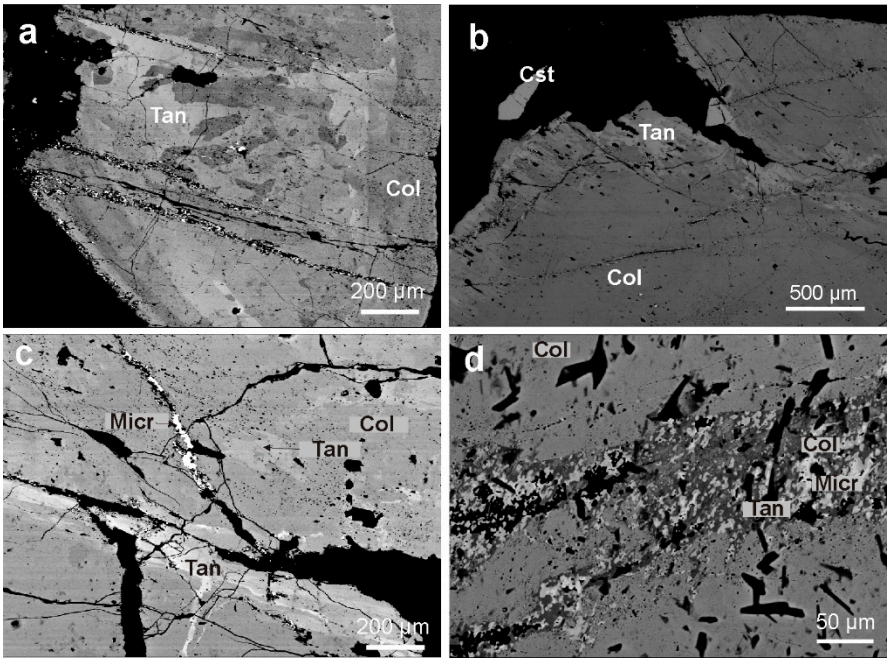

Figure 13. Textural patterns of Nb-Ta minerals from type-V pegmatites. SEM images, mode BSE. (**a**) fine-grained microlite (bright dot areas) in veins developed in a CGM crystal with patchy zoning, with Ta-rich areas (Tan) and Nb-rich ones (Col). (**b**) detail of a late replacement of columbite (col) by tantalite (tan), (**c**) microlite (Micr) and tantalite (tan) veins in CGM crystal with patchy zoning (col, columbite; tan, tantalite); (**d**) detail of the vein filling and replacement of a columbite crystal (Col) by tantalite (tan), microlite (Micr) and Ta-poor columbite (Col).

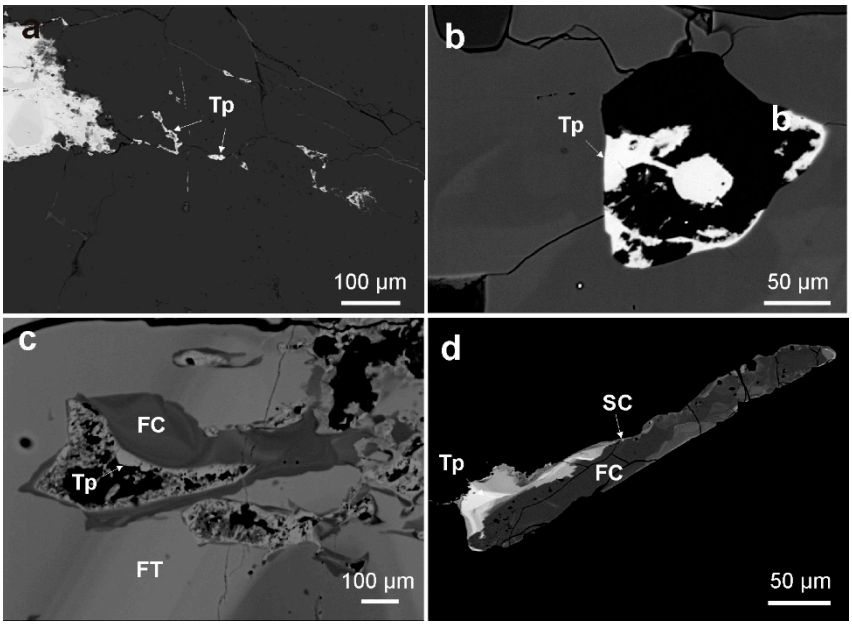

Figure 14. Textural patterns of tapiolite from type-IV pegmatites. (**a**) Tapiolite (Tp) filling fractures in quartz. (**b**) Tapiolite (Tp) filling a void in quartz produced by dissolution of a pre-existing mineral. (**c**,**d**) Replacement of columbite-(Fe) (FC) by tapiolite (TP) and stibiocolumbite (SC).

4.1.3. Textural Patterns of Cassiterite

Cassiterite appears only in type-IV and type-V pegmatites. In type-IV pegmatites, it is scarce and forms homogeneous hemihedral crystals in albite veins, up to 200 µm in size. Cassiterite is abundant

in all zones of type V pegmatite as idiomorphic crystals up to 1 mm in size; in this case, under the microscope, an oscillatory zoning is frequently observed. Some crystals are twinned to form the typical peak twin (Figure 15).

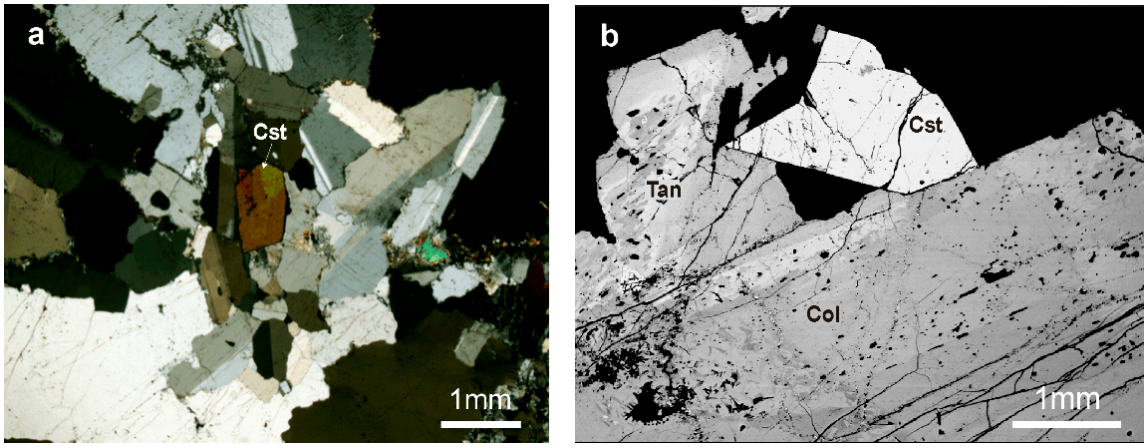

Figure 15. Cassiterite from type-V pegmatites. (**a**) Zoned crystal of cassiterite associated with quartz and albite in albite veins; (**b**) Twinned crystal of cassiterite associated with columbite and tantalite.

4.2. Mineral Chemistry

4.2.1. Zircon

Representative zircon compositions are presented in Table 1. The Hf content in type-I pegmatites is low, and appears relatively homogeneous within the crystal, ranging from about 2 to 4 wt.% HfO_2 (Figure 16a). These values are typical of slightly evolved granitic melts. The content in Th and U, is significant, thus explaining the metamict character to these zircon crystals.

Zircon crystals from granitic rocks in the study area are Hf-poor, although the Hf content increases from Ca-rich granitic rocks (less than 2 wt.% HfO_2) to the most evolved leucogranites (up to 4 wt.% HfO_2). Similar values are recorded in type-I pegmatites (less than 3 wt.% HfO_2). Hf contents are also low in zircon of the type-II pegmatites in the range 1–4 wt.% HfO_2). The content in Hf increases from the first to the second intermediate zone (Figure 16b). The zircon crystals of type-III pegmatites have relatively low Hf contents, as is typical in poorly evolved granitic magmas. Hafnon appears to be relatively homogeneously distributed within the crystal. The content in Hf increases from the earlier to the latest units, and their values are between 1–6% by wt.% HfO_2 (Figure 16c).

The composition of zircon in type-IV pegmatites varies according to the unit of the pegmatite. A complete sampling allows to appreciate the progressive decrease of the Zr/Hf ratio as the pegmatite crystallizes, that is, from the border zone to the third intermediate zone. In this way, zircon has values close to 1 wt.% HfO_2 in the border zone, to close than 4 wt.% in the first intermediate zone and, finally, up to about 12 wt.% HfO_2 in the second intermediate zone (Figure 16c). On the other hand, at the crystal level, the Hf content tends to increase slightly from the core to the rim. The Th content is below the detection limit of the electron microprobe. The content of U is maximum in the second intermediate zone; where the largest proportion of zircon is found. In addition, the content of U is also variable according to the zonation of the crystal; the highest values are located in the central part of the crystals, which is usually the most strongly metamict area.

In type-V pegmatites, the zircon crystals show a marked enrichment from the contact of the pegmatite with the host rock and the intermediate zones. In the intermediate zones, the Hf content increases considerably. These values are among the highest in the pegmatite field, indicating a moderate degree of fractionation (Table 1, Figure 16d). Zircon crystals are slightly zoned, with a slightly higher proportion of Hf toward the rim.

Table 1. Representative chemical composition (wt.%) of zircon from the Giraúl pegmatites.

Type	I	II	III	III	III	IV	IV	IV	V	V
Zone	1st I	1st I	1st	2nd I	3rd I	Border	1st	2nd I	Border	3rd I
Sample	X2B	GP13	Ibep3	I + 4B	pa8–4	a21–10	a6a	A10ap17	k100q	K100C
SiO_2	31.22	31.57	32.27	31.67	30.91	31.13	31.75	31.15	31.21	31.03
TiO_2	0.02	0.00	0.01	0.02	0.00	0.03	0.05	0.04	0.03	0.00
ZrO_2	61.38	65.86	65.29	63.17	63.71	64.72	60.33	56.93	67.05	56.12
HfO_2	2.56	2.15	1.39	3.32	4.69	1.68	5.66	11.89	1.38	11.54
ThO_2	0.00	0.00	0.07	0.04	0.08	0.00	0.00	0.04	0.09	0.00
Al_2O_3	0.53	0.00	0.00	0.00	0.00	0.05	0.25	0.02	0.00	0.00
Y_2O_3	0.29	0.17	0.10	1.38	0.00	0.21	1.31	0.00	0.00	0.00
U_2O_3	0.88	0.12	0.16	0.00	0.35	0.17	0.00	0.01	0.00	0.00
CaO	0.05	0.01	0.02	0.03	0.00	0.10	0.21	0.00	0.03	0.09
FeO	2.07	0.07	0.26	0.01	0.03	0.42	0.15	0.00	0.16	0.09
Total	99.91	99.95	99.57	99.64	99.77	98.51	99.71	100.08	99.95	98.87
					Apfu *					
Si	0.53	0.98	1.00	0.99	0.97	0.98	1.00	1.00	0.97	1.00
Zr	0.51	1.00	0.98	0.96	0.98	0.99	0.92	0.89	1.01	0.89
Hf	0.01	0.02	0.01	0.03	0.04	0.02	0.05	0.11	0.01	0.11
Al	0.01	0.00	0.00	0.00	0.00	0.00	0.01	0.00	0.00	0.00
Y	0.00	0.00	0.00	0.02	0.00	0.00	0.02	0.00	0.00	0.00
U	0.92	0.00	0.00	0.00	0.00	0.00	0.00	0.00	0.00	0.00
Ca	0.00	0.00	0.00	0.00	0.00	0.00	0.01	0.00	0.00	0.00
Fe	0.03	0.00	0.01	0.00	0.00	0.01	0.00	0.00	0.00	0.00
Zr/Hf	40.96	52.33	80.24	32.50	23.21	65.81	18.21	8.18	83.00	8.31

* Calculated on the basis of 2 cations pfu.

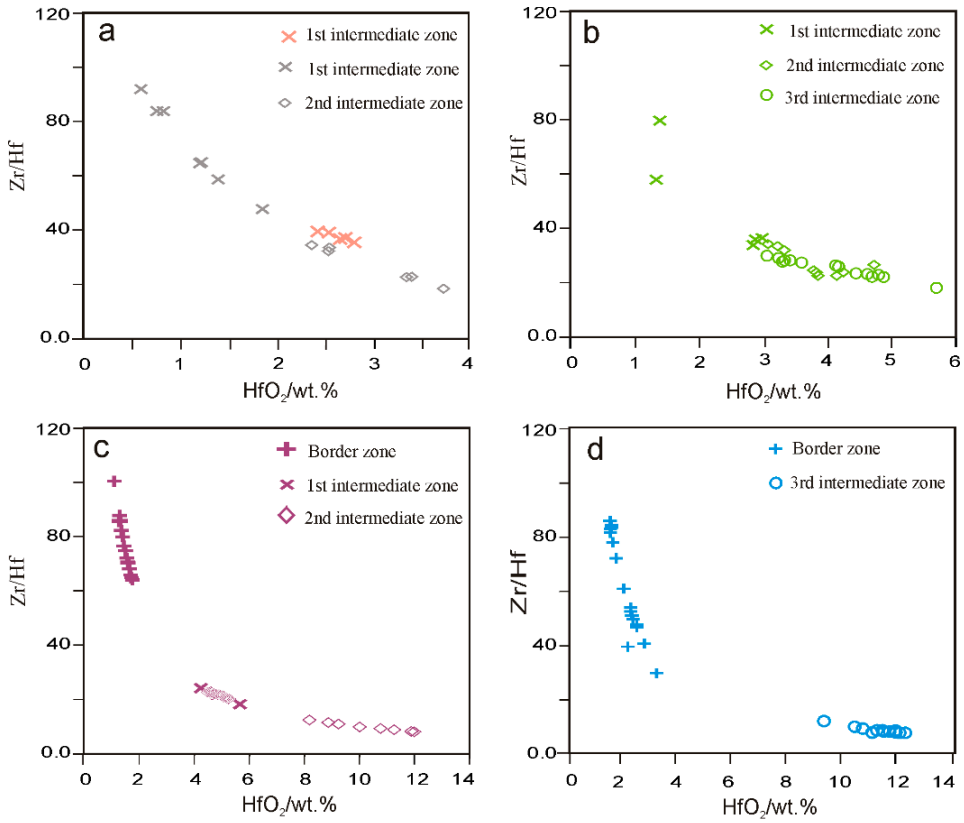

Figure 16. Zr/Hf vs HfO_2 in the Giraúl pegmatites (**a**) type I, orange, and II, grey, (**b**) type III, (**c**) type IV, (**d**) type V.

4.2.2. Columbite-Group Minerals

Columbite-group minerals from type-II pegmatites present an intermediate composition, with a Ta/(Ta + Nb) ratio from 0.52 to 0.64 and limited variation in the Mn/(Mn + Fe) ratio from 0.30 to 0.50 (Table 2).

Table 2. Representative chemical composition of CGM from the Giraúl pegmatites. FT, Tantalite-(Fe); MC, columbite-(Mn); FC, columbite-(Fe); MT, tantalite-(Mn).

Type	II	III	III	III	IV	IV	IV	IV	V	V	V	V	V
Zone	2nd I	3rd I	3rd I	3rd I	1st I	1st I	2nd I	2nd I	1st I	1st I	2nd I	3rd I	3rd I
Sample	GP1	PA8	P8	P8	D1e	A41c	A9Db	A10F	k40	k40	K100C	K100L	K100R
Mineral	FT	MC	MC	MT	MT	FC	MT	FC	FC	FC	FC	FC	FC
WO_3	0.30	2.40	0.52	0.40	n.a.	1.49	0.35	0.00	0.67	0.50	n.a.	1.03	1.08
Ta_2O_5	53.32	10.81	24.61	56.93	52.26	9.28	58.75	12.65	26.35	42.03	39.97	26.62	11.86
Nb_2O_5	27.08	65.53	54.93	25.06	29.34	68.25	24.29	67.16	52.86	39.65	41.70	52.20	64.86
TiO_2	0.29	1.70	0.95	0.51	1.23	1.23	0.26	0.22	0.87	0.33	0.32	1.05	1.77
UO_2	0.02	0.13	0.00	0.03	n.a	0.12	n.a.	0.08	0.07	n.a.	0.00	n.a.	n.a.
Y_2O_3	0.00	n.a.	n.a.	n.a.	0.01	0.09	n.a.	1.02	n.a.	n.a.	0.37	0.73	0.72
SnO_2	0.10	0.38	0.20	0.26	0.01	0.14	0.21	0.05	0.57	0.17	0.16	0.24	0.07
Fe_2O_3	0.63	0.00	0.00	0.00	0.01	0.00	0.00	0.06	0.00	0.00	0.00	0.70	1.71
FeO	8.13	9.00	8.75	7.48	7.79	14.48	2.71	14.04	13.24	9.43	10.49	14.19	14.53
MnO	7.57	10.28	9.11	7.74	8.46	4.65	12.71	5.50	4.79	7.60	6.90	3.59	3.69
MgO	0.00	0.03	0.03	0.16	n.a.	0.06	0.03	n.a.	0.04	0.00	n.a.	0.13	0.18
Sb_2O_3	0.00	0.00	0.00	0.00	0.00	0.02	0.00	0.06	0.00	0.00	0.00	0.00	0.00
PbO	0.00				0.18								
Total	97.44	100.26	99.10	98.57	99.29	99.81	99.31	100.78	99.46	99.71	99.91	100.48	100.47
					Atomic contents								
W^{6+}	0.023	0.019	0.034	0.031	-	0.090	0.027	-	0.044	0.035	-	0.067	0.065
Ta^{5+}	4.268	0.699	1.675	4.556	4.046	0.589	4.715	0.808	1.806	3.092	2.904	1.805	0.750
Nb^{5+}	3.604	7.049	6.214	3.334	3.776	7.196	3.240	7.132	6.024	4.848	5.037	5.883	6.822
Ti^{2+}	0.064	0.304	0.179	0.113	0.263	0.216	0.058	0.039	0.165	0.067	0.064	0.197	0.310
U^{4+}	0.001	0.007	0.000	0.002	-	0.006	-	0.004	0.004	-	0.000	-	-
Y^{3+}	0.000	-	-	-	0.002	0.011	-	0.128	-	-	0.053	0.097	0.089
Sn^{4+}	0.012	0.036	0.020	0.034	0.001	0.013	0.025	0.005	0.057	0.018	0.017	0.024	0.006
Fe^{3+}	0.140	0.000	0.000	0.000	0.002	0.000	0.000	0.000	0.000	0.000	0.000	0.131	0.299
Fe^{2+}	2.001	1.791	1.831	1.841	1.855	2.824	0.669	2.758	2.791	2.133	2.344	2.958	2.827
Mn^{2+}	1.887	2.072	1.931	1.929	2.040	0.919	3.177	1.094	1.023	1.741	1.562	0.758	0.727
Mg^{2+}	0.000	0.018	0.019	0.116	-	0.035	0.022	-	0.025	0.000	0.000	0.080	0.104
Sb^{3+}	0.000	0.000	0.000	0.000	0.000	0.002	0.000	0.006	0.000	0.000	0.000	0.000	0.000
Pb^{2+}	0.000	0.000	0.000	0.000	0.014	0.000	0.000	0.000	0.000	0.000	0.000	0.000	0.000
CATSUM	12.000	11.994	11.901	11.955	12.000	11.901	11.932	11.974	11.940	11.935	11.981	12.000	12.000
Ta/(Ta + Nb)	0.542	0.090	0.212	0.577	0.517	0.076	0.593	0.102	0.231	0.389	0.366	0.235	0.099
Mn/(Mn + Fe)	0.469	0.536	0.513	0.512	0.523	0.245	0.826	0.284	0.268	0.449	0.400	0.197	0.189

n.a.: not analysed.

Zoned crystals of columbite-group minerals from type-III pegmatites correspond to columbite-(Fe) and tantalite-(Fe), reaching locally to be tantalite-(Mn) (Figure 17). In this case, the Ta/(Ta + Nb) ratio varies between 0.13 and 0.58, and the Mn/(Mn + Fe) ratio between 0.39 and 0.58. The non-zoned crystals consist of columbite-(Fe), with Ta/(Ta + Nb), between 0.8 and 0.11, whereas the Mn/(Mn + Fe) ratio ranges between 0.34 and 0.54. The content of TiO_2 usually ranges from 1.2 to 2.11 wt.%. The amount of WO_3 is between 0.22 and 2.31 wt.%, SnO_2 is less than 0.6 wt.% and MgO is in the rang 0.01–0.16 wt.%. Other elements such as Y and Sb are below the detection limit.

Type-IV pegmatites have a large compositional range in the contents of Nb and Ta, as observed in the columbite quadrilateral, where the composition of these minerals has been represented (Figure 17). Crystals of CGM in some of these pegmatites are euhedral, up to 5 cm in length, with no zonation observable. Its chemical composition is very homogeneous, consisting of columbite-(Fe) poor in Ta and Mn; the Mn/(Mn + Fe) ratio is 0.04 and Ta/(Ta + Nb) is in the range 0.08–0.09. They contain between 0.8 and 1.2 wt.% TiO_2 and up to 0.4 wt.% PbO. Other components (W, Sn, U, Y, Sb) at low levels.

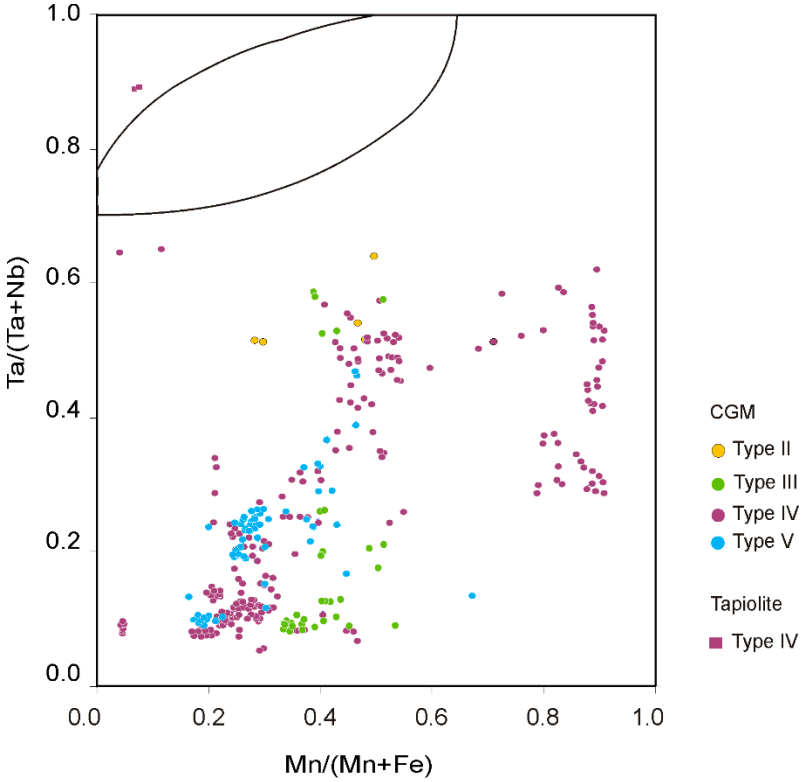

Figure 17. Composition of the CGM (dots) and tapiolite (square) from the Giraúl pegmatites in terms of the columbite quadrilateral (atomic ratios).

Columbite-group minerals from the largest mined type-IV pegmatite are characterized by intermediate composition both in the Ta/(Ta + Nb) ratio and in the Mn/(Mn + Fe) ratio (Figures 16 and 18a). They can have up to 2.7 wt.% TiO_2. Other components, as in the type-III pegmatites, are very low. In this pegmatite the CGM occur in the first and second intermediate zones. Crystals of the CGM from the first intermediate zone have values of Ta/(Ta + Nb) between 0.2 and 0.3; Mn/(Mn + Fe) values range between 0.18 and 0.8, therefore extend into the columbite-(Mn) field. In the vicinity of the contact with the second intermediate zone, the crystals present a zoning characterized by a Ta-rich rim (Figure 9b), with values of Ta/(Ta + Nb) between 0.11 and 0.28; the ratio Mn/(Mn + Fe) ranges from 0.23 to 0.35. The highest values in Ta/(Ta + Nb) and in Mn/(Mn + Fe) ratios were found in crystals of the second intermediate zone. In this zone, the Nb-Ta crystals have distinct characteristics in terms of composition. Three groups can be established. A first group are columbite-(Fe) crystals with a homogeneous composition poor in Ta; the Ta/(Ta + Nb) ratio is 0.06–0.15, and the Mn/(Mn+Fe) ratio, 0.21–0.30. The second are crystals with a convoluted zoning and composition ranging from columbite-(Fe) to tantalite-(Fe); the Ta/(Ta + Nb) ratio is from 0.24 to 0.57 and Mn/(Mn + Fe) ratio is in the range 0.34–0.44 (Figure 9c,d). The third are crystals with a convoluted zoning in the central part, surrounded by a rim with concentric oscillatory zones, with a composition ranging from columbite-(Fe) to columbite-(Mn); the (Ta/(Ta + Nb) ratio is 0.29 to 0.59 and Mn/(Mn + Fe) ratio is 0.72 to 0.89 (Figure 9e,f). Late overgrowths of CGM have the highest Ta/(Ta + Nb) and Mn/(Mn + Fe) values, up to 0.65 and 0.9, respectively.

In other cases of type-IV pegmatites, TiO_2 tends to behave inversely to that of the Ta/(Ta + Nb) ratio. However, the CGM of a pegmatite body are characterized by higher TiO_2 contents than those that should be expected for its content in Ta (Figure 11).

Columbite-group minerals in type-V pegmatite have Ta/(Ta + Nb) values oscillating mostly between 0.10 and 0.24, whereas the Mn/(Mn + Fe) ratios are between 0.16 and 0.45 (Figures 16 and 18b). There is a single exception in an analysis corresponding to the third intermediate zone, where the

Mn/(Mn + Fe) reaches 0.65 and, therefore, it is columbite-(Mn). Amounts of WO_3, TiO_2 and SnO_2 are usually less than 1 wt.%; Sb, Pb, Ca, Mg and Bi are found in trace concentrations.

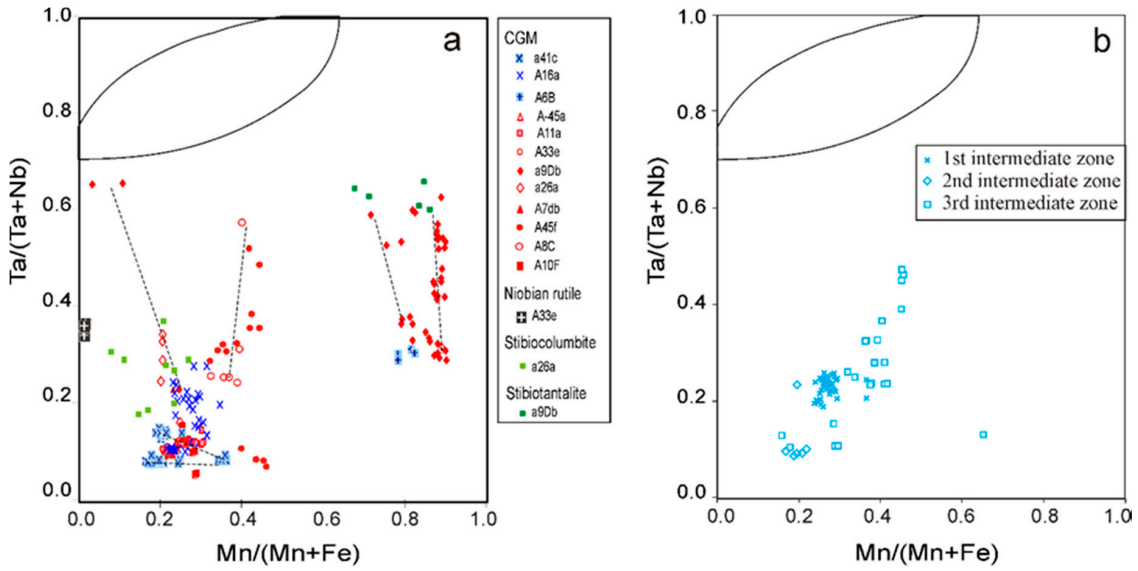

Figure 18. Composition of the Nb-Ta rich minerals plotted in the columbite quadrilateral (atomic ratios) of (**a**) type IV pegmatites; blue, first intermediate zone and red, second intermediate zone; (**b**) type-V pegmatites. Dashed lines represent the composition of different areas in the same crystal.

4.2.3. Stibiocolumbite and Stibiotantalite

In type-IV pegmatites, stibiocolumbite and stibiotantalite are present in small veins replacing other Nb-Ta oxides. These minerals are characterized by Ta contents higher than the Nb-Ta oxides that they replace. However, they have very low contents in Mn; their Mn/(Mn + Fe) values are similar to those of the replaced Nb-Ta oxides. This higher content in Ta is contrary to that found in other locations, where the values of both groups of minerals are similar [44]. The content of Sb_2O_3 varies between 40 and 48 wt.%; Y_2O_3 is in the range 2.6–3.4 wt.% and Bi_2O_3 is less than 0.08 wt.%.

4.2.4. Pyrochlore Supergroup

The pyrochlore supergroup can be described by the general formula A_{2-m} B_2 X_{6-w} Y_{1-n} [45]. The B site can be occupied by Ti, Nb and Ta; Nb and Ta are the dominant cations in the Giraúl suite. According to the B site occupancy, in all cases of type_III pegmatites and most of the type-IV pegmatites, pyrochlore-supergroup minerals belong to pyrochlore *ss*, although the Ta/(Ta + Nb) in pyrochlore is invariably higher than that of the host replaced columbite. On the contrary, microlite is the dominant pyrochlore-group mineral in type-V pegmatites (Figure 19), where it occurs as crystals included in tantalite with the composition in Mn/(Mn + Fe) highest of the entire pegmatite field.

The amount of TiO_2 oscillates between 1.5 and 3.2 wt.% except in some pyrochlore minerals of type-IV pegmatites, where it ranges between 4.2 and 6.2 wt.%. In type-V pegmatites, TiO_2 can attain up to 10 wt.%, and WO_3 attains up to 2.6 wt.%.

The A site can be occupied mainly by Na, Ca, Bi, U, Pb, REE and vacancies. The Y position is occupied by O, OH, F and vacant positions. In type-III pegmatites, Bi, U and Pb are dominant with respect to Ca and Na, which are the most abundant in type-V pegmatites (Figure 20). The members of this supergroup are classified according to the occupancy of the B, A and Y positions [45]. A wide variety in the cations of A site occurs in the Giraúl pegmatites (Table 3).

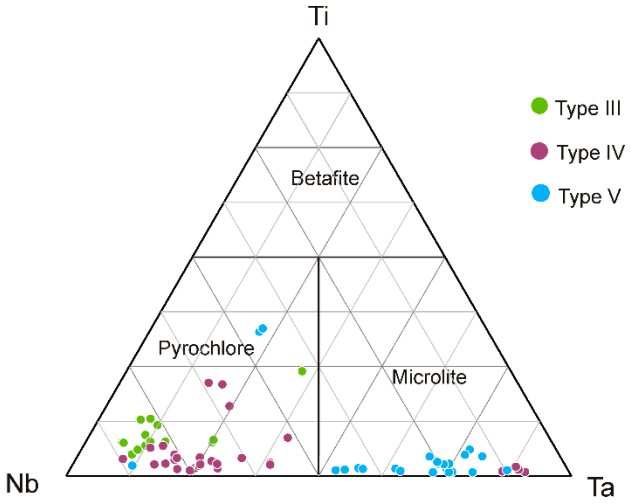

Figure 19. Nb-Ta-Ti compositional plot of the pyrochlore-supergroup minerals from the Giraúl pegmatites. Black solid lines after [45].

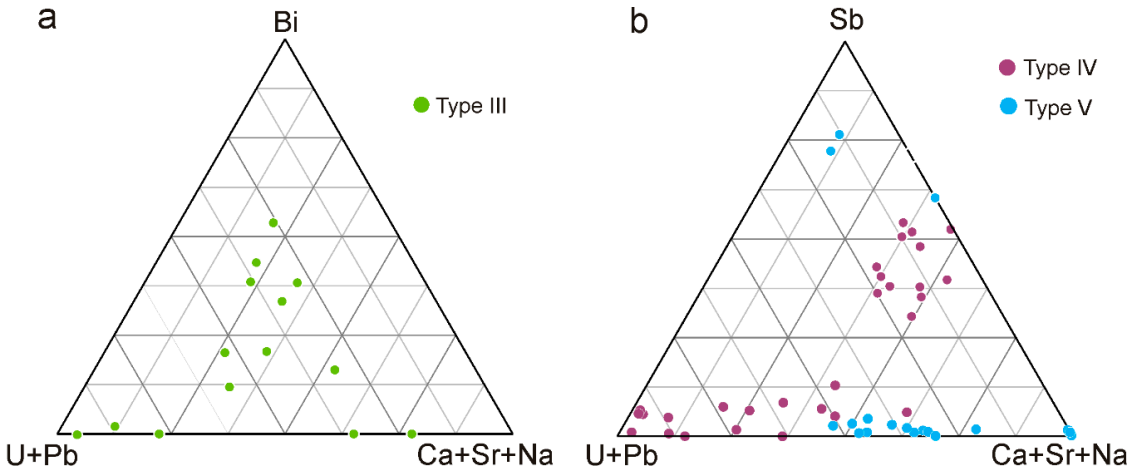

Figure 20. Compositional plot of the pyrochlore-supergroup minerals from the Giraúl pegmatites. (**a**) U + Nb – Bi – Ca + Sr + Na; (**b**) U + Nb – Sb – Ca + Sr + Na.

The Bi content is only significant in type-III pegmatites, where it reaches up to 21.0 wt.% Bi_2O_3. Bismuth is the dominant cation at the A position, approaching it to the bismutocolumbite end-member. Where there are high contents in Bi, the sum of the total of oxides is less than 89 wt.%. However, in the presence of any other element was not detected in the EDS spectra, which suggests the presence of high contents of H_2O. This is probable, as in the holotype of bismutocolumbite from the Mika pegmatite, in the Pamirs Mountains, the amount of H_2O is close to 14.6 wt.% [46].

The content in UO_2 is variable, up to 36.5 wt.%. The content of PbO oscillates between 7 wt.% and 46.11%. In detail, there is a negative correlation between Pb and U, as can be seen in the distribution map of elements (Figure 21).

In these cases, CaO and Na_2O are significantly low. The contents in Sb, Y and Sr are negligible; BaO, Na_2O and K_2O are generally less than 0.2 wt.% and there is a high proportion of vacant positions in the A site. These characteristics are typical of secondary pyrochlore [47]. Similar values were reported in pyrochlore supergroup minerals that were partly transformed to liandratite [48]. Low Ca and alkali contents in secondary pyrochlore can also be coupled with enrichments in Sb, up to 25.1–25.9 wt.% Sb_2O_3. Thorium and Y occur invariably in minor amounts. Manganese and Fe generally present values lower than 1 wt.% except one grain of pyrochlore, with 8 wt.% Fe_2O_3.

Table 3. Chemical composition, wt.%, of pyrochlore-supergroup minerals from the Giraúl pegmatites.

Type	**III**	**III**	**III**	**IV**	**IV**	**V**	**V**	**V**	**V**
Mineral	OBP	HPP	OUP	HPP	HKP	FNM	ONM	FNM	HSP
Sample	P-5	P-10	P-11	A33b	A11A	K100-20	K100C46	K100C32	K100L
WO_3	0.00	2.59	0.79	1.10	4.14	n.a.	n.a.	n.a.	1.19
Nb_2O_5	35.04	16.37	30.16	26.59	45.49	18.53	11.24	25.40	24.23
Ta_2O_5	5.23	22.86	5.32	18.20	17.80	58.29	55.74	48.42	19.45
TiO_2	1.88	5.70	2.96	4.40	1.11	0.40	0.71	0.30	10.51
SnO_0	0.31	0.72	0.38	0.17	0.24	0.19	3.08	0.29	0.72
ThO_2	0.00	n.a.	n.a.	0.07	0.00	n.a.	n.a.	n.a.	0.00
UO_2	8.39	0.00	36.31	1.90	0.08	0.15	14.88	0.25	0.00
Sc_2O_3	0.00	0.06	0.11	0.10	0.36	n.a.	n.a.	n.a.	0.32
Y_2O_3	0.23	0.00	0.00	n.a.	0.80	0.00	0.00	0.31	0.00
Sb_2O_3	0.34	0.60	0.00	0.48	19.98	0.55	0.65	0.92	25.92
Bi_2O_3	21.04	0.00	0.00	n.a.	0.00	0.04	0.20	0.00	0.00
CaO	1.73	1.07	2.19	0.03	0.00	9.50	5.65	10.45	0.03
MnO	0.56	0.69	0.48	0.15	0.11	0.17	0.00	0.14	0.10
FeO	4.35	1.56	1.84	1.09	0.55	0.65	0.04	0.40	1.32
SrO	0.00	0.00	0.00	n.a.	0.00	2.71	0.85	1.96	0.81
BaO	0.13	n.a.	n.a.	0.14	0.00	n.a.	n.a.	n.a.	0.00
PbO	3.06	46.11	8.37	44.56	0.29	0.09	1.34	0.08	9.34
Na_2O	0.05	0.22	0.20	0.14	3.72	5.52	3.87	6.47	0.56
K_2O	0.16	0.00	0.19	0.03	0.14	0.00	0.01	0.05	0.00
F	0.01	0.00	0.30	0.23	0.00	5.23	0.79	5.84	0.16
OH		1.19	0.00	2.12	2.79	0.00	0.18	0.00	1.95
O=F	−0.01	0.00	−0.15	−0.12	0.00	−2.62	−0.40	−2.92	−0.08
Total	82.51	99.74	89.45	101.38	97.60	99.40	98.84	98.36	96.53
					apfu				
W^{6+}	0.000	0.077	0.025	0.030	0.084	-	-	-	0.027
Nb	1.696	0.795	1.555	1.168	1.501	0.683	0.489	0.923	0.895
Ta	0.152	0.668	0.165	0.481	0.353	1.292	1.460	1.059	0.432
Ti	0.151	0.460	0.254	0.321	0.061	0.025	0.051	0.018	0.646
ΣB site	2.000	2.000	2.000	2.000	2.000	2.000	2.000	2.000	2.000
Sn^{4+}	0.015	0.035	0.019	0.007	0.008	0.007	0.132	0.010	0.026
Th	0.000	-	-	0.002	0.000	-	-	-	0.000
U	0.200	0.000	0.922	0.041	0.001	0.003	0.319	0.004	0.000
Sc	0.000	0.006	0.011	0.008	0.023	-	-	-	0.023
Y	0.013	0.000	0.000	0.000	0.031	0.000	0.000	0.013	0.000
Sb	0.015	0.027	0.000	0.019	0.601	0.018	0.026	0.030	0.873
Bi	0.581	0.000	0.000	0.000	0.000	0.001	0.005	0.000	0.000
Ca	0.198	0.123	0.268	0.003	0.000	0.830	0.583	0.900	0.003
Mn^{2+}	0.051	0.063	0.046	0.012	0.007	0.012	0.000	0.010	0.007
Fe^{2+}	0.389	0.140	0.176	0.089	0.034	0.044	0.003	0.027	0.090
Sr	0.000	0.000	0.000	-	0.000	0.128	0.047	0.091	0.038
Ba	0.006	-	-	0.005	0.000	0.000	0.000	0.000	0.000
Pb	0.088	1.333	0.257	1.165	0.006	0.002	0.035	0.002	0.205
Na	0.010	0.046	0.044	0.026	0.527	0.873	0.723	1.009	0.089
K	0.022	0.000	0.028	0.004	0.013	0.000	0.001	0.005	0.000
ΣA site	1.589	1.772	1.770	1.382	1.250	1.917	1.874	2.102	1.354
F	0.003	0.000	0.108	0.071	0.000	1.348	0.241	1.485	0.041
OH	0.000	0.853	0.000	1.375	1.360	0.000	0.116	0.000	1.064
oxygen	6.997	6.147	7.492	5.554	5.640	5.807	6.644	5.871	5.895
ΣYsite	7.000	7.000	7.600	7.000	7.000	7.155	7.000	7.356	7.000

OBP, "oxybismutopyrochlore"; HPP, "hydroplumbopyrochlore"; OUP, "oxyuranpyrochlore"; HKP, hydrokenopyrochlore; FNM, fluornatromicrolite, ONM, oxynatromicrolite; HSP, "hydrostibiopyrochlore".

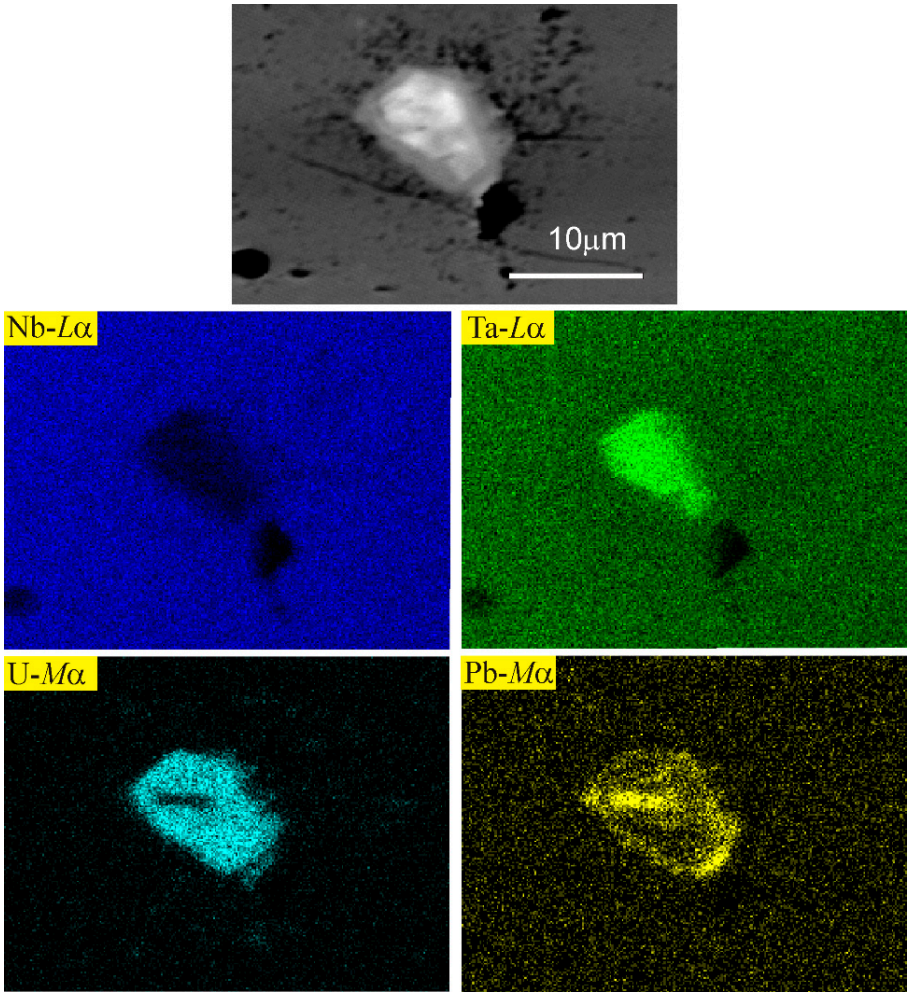

Figure 21. BSE images and elemental maps for a zoned grain of microlite replacing columbite. U-rich microlite is replaced by Pb-rich microlite.

Finally, the Y site can be mainly occupied by F, OH and oxygen. The F content is between 0 and 6.16 wt.% in the Giraúl pegmatites, being high only in the microlite group from type V pegmatites. Microlite from the Giraúl pegmatites is mainly fluornatromicrolite in type-V and oxynatromicrolite in the rest (Table 3).

Two generations of microlite are distinguished in type-V microlite with a marked difference between the compositions of the two. One of them is rich in Ca (9.5–11.0 wt.% CaO), Na (5.5–6.5 wt.%) and fluorine (4.9–6.2 wt.%). The other is rich in U, with 13.0–16.0 wt.% UO_2, up to 3 wt.% PbO, and up to 1.5 wt.% F.

4.2.5. Rutile Group

Minerals of the rutile group only occur in type-IV pegmatites, where niobian rutile appears in the second intermediate zone of some pegmatites. The Ta/(Ta + Nb) can be high enough to be named as tantalian rutile (Table 4). The ratio Mn/(Mn + Fe) is usually very low may reach up to 0.33. The Fe and Mn contents are correlated with Nb and Ta. The WO_3 content can be high, up to 3.36 wt.% WO_3. Similar contents have been reported in pegmatites from the Písek region, Czech Republic [49].

Table 4. Representative chemical composition (wt.%) of niobian rutile (Nbrt) and tantalian rutile (Tart) from the Type-IV pegmatites.

Zone	**1st I**		**2nd I**			
Sample	A33a	A33b	D1E	D1E	D1E	D1E
Mineral	Nbrt	Nbrt	Nbrt	Nbrt	Nbrt	Tart
WO_3	n.a.	n.a.	3.36	1.89	1.08	2.40
Nb_2O_5	7.35	10.32	21.56	13.32	16.79	9.78
Ta_2O_5	6.90	8.94	33.47	19.87	10.54	26.14
TiO_2	79.94	74.20	28.48	55.81	62.88	49.17
SnO_2	0.00	0.00	0.00	0.04	0.00	0.05
UO_2	0.00	0.00	0.12	0.01	0.09	0.05
Y_2O_3	0.00	0.00	0.04	0.00	0.14	0.43
MgO	0.00	0.00	0.10	0.02	0.02	0.15
MnO	0.02	0.03	4.35	0.31	0.33	1.19
Fe_2O_3	4.80	5.33	9.85	9.72	9.18	10.23
Total	99.01	98.82	101.33	100.99	101.05	99.59
			apfu			
W^{6+}	-	-	0.052	0.025	0.014	0.034
Nb	0.144	0.207	0.542	0.288	0.344	0.224
Ta	0.081	0.108	0.506	0.259	0.130	0.360
Ti	2.601	2.473	1.192	2.008	2.140	1.875
Sn^{4+}	0.000	0.000	0.000	0.001	0.000	0.001
U^{4+}	0.000	0.000	0.001	0.000	0.001	0.001
Y^{3+}	0.000	0.000	0.001	0.000	0.003	0.012
Mg	0.000	0.000	0.008	0.001	0.001	0.011
Mn^{2+}	0.001	0.001	0.205	0.013	0.013	0.051
Fe^{3+}	0.156	0.178	0.413	0.350	0.313	0.391
Cat.Sum	2.983	2.966	2.921	2.945	2.958	2.960

4.2.6. Cassiterite

Cassiterite, in addition to Sn, contains Ta, Ti, Fe, Mg, and in smaller amounts, Nb and Mn (Table 5). Tin can be replaced by Nb, Ta and Ti. Niobium always is scarce; the most important minor element is Ta, which can reach up to 5.53 wt.% Ta_2O_5. Ti content is significant in type-IV pegmatites and in some crystals of the third intermediate zone of type-V pegmatites (Figure 22). The content in Fe is invariably higher than that of Mn; the Mn/(Mn + Fe) ratio in most cases is less than 0.20.

The contents of these elements were interpreted by some authors as due to micro-inclusions of Nb-Ta minerals that are the product of exsolution processes or trapped crystals [50]. In order to verify if this is what happens in cassiterite [51,52], use the scheme of substitution $(Fe, Mn)^{2+} + 2(Nb, Ta)^{5+} \leftrightarrow 3(Sn, Ti)^{4}$. This is the case of most cassiterite from type-V pegmatites the Giraúl field. However, in the third intermediate zone of type IV pegmatites, Ti has the same behaviour as Nb and Ta. The substitution would be $(Fe, Mn)^{2+} + 2(Nb, Ta, Ti) \leftrightarrow 3Sn^{4+}$ (Figure 22c). The correlation between these groups of elements defines a (Fe + Mn)/(Ta + Nb + Ti) ratio of 1:2, which is the value of the ideal columbite-group composition. The micro-inclusions in the case of type-IV pegmatites can be attributed to ilmenite and tantalian rutile, whereas in the cassiterite of type-V pegmatite, they mainly are tantalian rutile and tapiolite (Figure 22d).

Table 5. Representative chemical composition (wt.%) of cassiterite from the Giraúl pegmatites.

Type	**IV**				**V**				
Zone	2nd I		1st I		2nd I		3rd I		
Sample	A11a	i4 + b	K40	K40	K100B	K100B	K100d	kK00d	K100L
WO_3	0.04	0.00	0.00	0.00	n.a.	n.a	0.3	0.53	0.19
Nb_2O_5	0.37	0.05	0.37	0.37	1.04	0.11	0.00	0.44	0.00
Ta_2O_5	0.79	0.38	2.32	1.79	5.53	3.38	0.98	3.76	0.19
TiO_2	0.23	1.32	0.2	0.26	0.13	0.08	0.08	0.12	0.27
SnO_2	98.59	98.48	96.53	97.32	91.63	95.51	99.48	95.68	99.36
UO_2	0.11	0.06	n.a	n.a	n.a.	n.a	n.a	0.00	0.00
MgO	0.20	0.18	0.05	0.08	0.09	0.05	0.17	0.12	0.14
MnO	0.08	0.04	0	0	0.04	0.07	0.05	0.06	0.00
Fe_2O_3	0.47	0.45	0.52	0.43	1.32	0.79	0.2	0.86	0.16
Total	100.88	100.97	99.99	100.25	99.78	99.99	101.26	101.57	100.31
					apfu				
W^{6+}	0.001	0.000	0.000	0.000	-	-	0.004	0.007	0.003
Nb	0.008	0.001	0.008	0.008	0.024	0.003	0.000	0.010	0.000
Ta	0.011	0.005	0.032	0.024	0.076	0.046	0.013	0.051	0.003
Ti	0.009	0.049	0.008	0.010	0.005	0.003	0.003	0.004	0.010
Sn^{4+}	1.948	1.927	1.930	1.938	1.842	1.917	1.963	1.888	1.974
U^{4+}	0.003	0.001	-	-	-	-	-	0.000	0.000
Mg	0.015	0.013	0.004	0.006	0.007	0.004	0.013	0.009	0.010
Mn^{2+}	0.003	0.002	0.000	0.000	0.002	0.003	0.002	0.003	0.000
Fe^{2+}	0.018	0.017	0.020	0.016	0.050	0.030	0.008	0.032	0.006
Cat, Sum	2.015	2.015	2.002	2.003	2.004	2.006	2.006	2.003	2.006

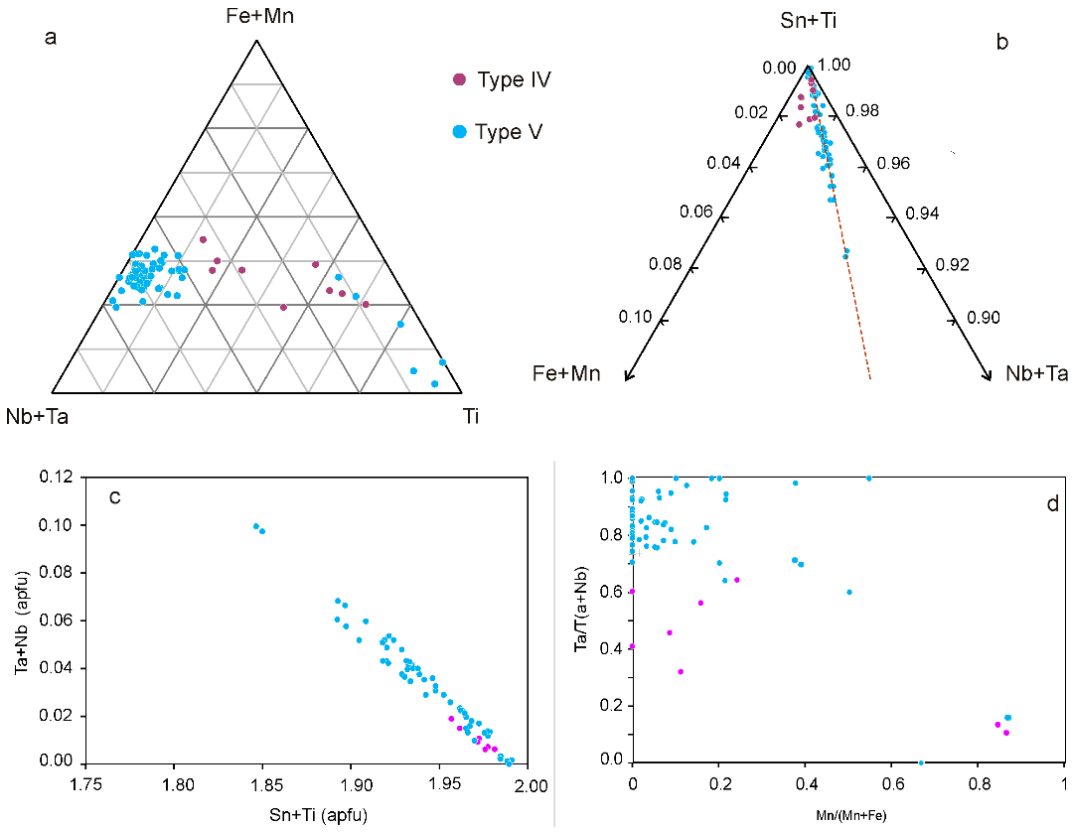

Figure 22. Cassiterite composition from the Giraúl pegmatites. (**a**) Fe + Mn – Nb + Ta – Ti diagram. (**b**) Fe + Mn – Sn + Ti – Nb + Ta diagram. (**c**) Sn + Ti vs Ta + Nb. (**d**) Ta/(Ta + Nb)/(Mn/(Mn + Fe) quadrilateral.

4.2.7. Uraninite

Uraninite occurs as micrometric inclusions in minerals of the columbite group in type-III and type-IV pegmatites, frequently together with minerals of the pyrochlore-supergroup. The compositional characteristics are similar in both cases. The content in UO_2 ranges between 76 and 87 wt.% by weight; the PbO between 4.6 and 10 wt.%, the Nb_2O_5 is 0.5–6.8 wt.%, Ta_2O_5, 0.8–1.5 wt.%. CaO up to 3.2 wt.%, Bi_2O_3 up to 0.9 wt.% and Th_2O_3 up to 1.7 wt.%.

5. Discusion

5.1. Evolution of Zircon in the Giraúl Pegmatites

Zircon is common to all pegmatites and granites of the area. In these minerals, the substitution of Zr by Hf can occur in variable proportions. The Hf contents in Giraúl pegmatites can be relatively high in some pegmatites, up to 12 wt.%, although never reaching proportions close to the field of hafnon ($HfSiO_4$) and clearly lower than those from other evolved pegmatite fields [53,54]. Extremely Hf-rich contents were reported with up to more than 48 wt.% Hf in the rare-metal pegmatites of the Vasin-Mylk deposit, in the Kola peninsula [55]. The content of Hf in zircon usually is correlated with the content of Ta in the CGM with which it is associated, thus, it is a good criterion in the exploration of rare elements [15,56–58]. Following this criterion, the potential for Ta of the Giraúl field is moderate.

However, in the Giraúl pegmatite field, the zircon crystals present wide variations depending on the pegmatite. In pegmatites of type I, II and III the maximum Hf contents are significantly lower than in type IV and V (Figure 23). Moreover, the zircon composition varies depending on the stage of crystallisation of the pegmatites. In every pegmatite type, the Hf/Zr ratio increases from the earliest to the latest crystallisation zones (Figure 16), which is in accordance with the higher solubility of Hf compared with Zr in pegmatite-forming melts [14,59].

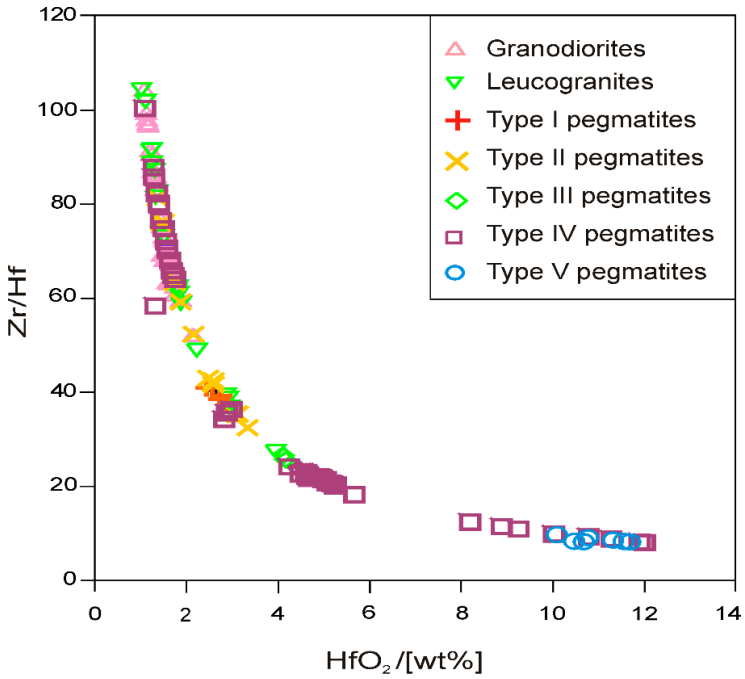

Figure 23. Evolution of the composition of the zircon crystals from the granitic rocks towards the most evolved pegmatites.

5.2. Evolution of the Nb-Ta Oxide Minerals in the Giraúl Pegmatites at Crystal Scale

Columbite-group minerals from the less evolved pegmatites of the Giraúl suite do not exhibit zoning. They may well represent growth from the melt phase. In other cases, the CGM crystals from the

granitic pegmatites present a great variety of zoning patterns. Both in type-III and type-IV pegmatites, the presence of a convoluted zoning in these crystals is frequent. In some cases a combination between convoluted zoning and oscillatory zoning occurs. Crystals with a concentric zoning around the convoluted zone seem to have formed at a late stage (Figure 12a–d). According to [60], this zonation can be due to an incomplete miscibility of the solid solution. In this case the total composition would be located in the immiscibility gap [61] of the CGM quadrilateral, and the minerals in contact should be columbite or tantalite and tapiolite [62].

Oscillatory zoning is common and Lahti [63] attributed this zoning to the growth dynamics of the crystals, changes in the concentration of the main elements and successive pulses of the magma According to Putnis et al. [64] where the solubility of two end members of a solid solution is significantly different, the supersaturation threshold for the nucleation of supersaturated solutions facilitates the oscillatory zoning, even in the absence of oscillations in the intensive parameters.

The convoluted zoning often occurs where CGM are affected by the action of late fluids. This replacement occurs at the rim of the crystals or through microfractures, producing a partial dissolution followed by a later crystallisation [28,63,65,66]. In some cases, as in the Cap de Creus pegmatites [28] and in the Penouta rare-element leucogranite [21], such convoluted zoning is attributed to metasomatism produced by late Na-rich fluids exsolved from the melt by an unmixing process. In other cases, external metamorphic fluids are involved, for example in the pegmatites of Marsikov, Czech Republic [67].

Where Nb-Ta oxide minerals occur in pegmatites that do not have a zonal internal structure, the Ta/(Ta + Nb) and Mn/(Mn + Fe) ratios are more constant. These pegmatites are characterized by high contents of CGM with limited variations of Mn, (Mn/(Mn + Fe) is around 0.5. This could be due to the fact that these pegmatites present high Ti contents, which, together with the CGM, form minerals of the rutile group, which preferably incorporate Fe into their structure, producing a buffer effect in the Mn/(Mn + Fe) ratio in the pegmatite fluid from which the CGM will precipitate. This effect explains the compositions of Nb-Ta minerals in some pegmatites from Separation Rapids, Canada [63]. The high content in Ti could be due to a contamination by the host rock. This has been suggested in other pegmatite fields [68,69]. Such contamination would have a more marked effect on the composition of a few number of pegmatites in the Giraúl field. Other components of these minerals, such as Sb and Bi, could also have been incorporated from the host rock.

In the pegmatites with a complex internal structure Nb-Ta minerals are characterized by the increase in the complexity of the mineralogy as the successive units are formed. First, the number of crystals increase and the textural complexity also increases, evolving from non-zoned or poorly-zoned crystals in the first intermediate zone to convoluted zonation in the second intermediate zone.

Second, the chemical composition becomes more complex, and the range of values in the Ta/(Ta + Nb) and Mn/(Mn + Fe) ratios increases. The lowest values in these relationships are found in the crystals of the first intermediate zone. Other crystals in this zone have values of Ta/(Ta + Nb) and Mn/(Mn + Fe) similar to those of the second intermediate zone. The highest values in these ratios occur in the late CGM generations, which are associated in addition with Ta-rich members of the rutile group, stibiotantalite, and pyrochlore supergroup. The last two also show a proportional increase in Ta/(Ta + Nb) ratio with respect to that found in the replaced columbite.

5.3. Evolution in the Composition of the Nb-Ta Oxides at Field Scale

One of the most important aspects in the study of Nb-Ta minerals in granitic pegmatites is that the composition of these minerals follows a trend with the evolution of the pegmatite that indicates its degree of evolution [65,68,70], The evolution of the different types of rare-element pegmatites follows a characteristic trend in the composition, which is represented in the quadrilateral of CGM.

In the Giraúl pegmatites, there is a tendency to increase the content of Nb-Ta minerals with the degree of evolution of the pegmatite, from type II to V. The Ta/(Ta + Nb) ratio does not vary significantly with the type of pegmatite (Figure 15).

In the case of type-II pegmatites, the activity of Nb and Ta is sufficiently high to form minerals only during the very late stages of formation of these pegmatites; therefore, the Ta/(Ta + Nb) and Mn/(Mn + Fe) ratios are relatively high in these cases.

Another important aspect in the Giraúl field is the development, even at the microscale, of minerals of the pyrochlore supergroup, all of them formed at very late stages of crystallisation and by replacement of the CGM. Although the Ta/(Ta + Nb) value is similar for pegmatites of types III, IV and V, and even somewhat higher in some type IV crystals, the minerals of the pyrochlore supergroup are enriched in Ta in the case of Type-V pegmatites, where they correspond to microlite (Figure 24).

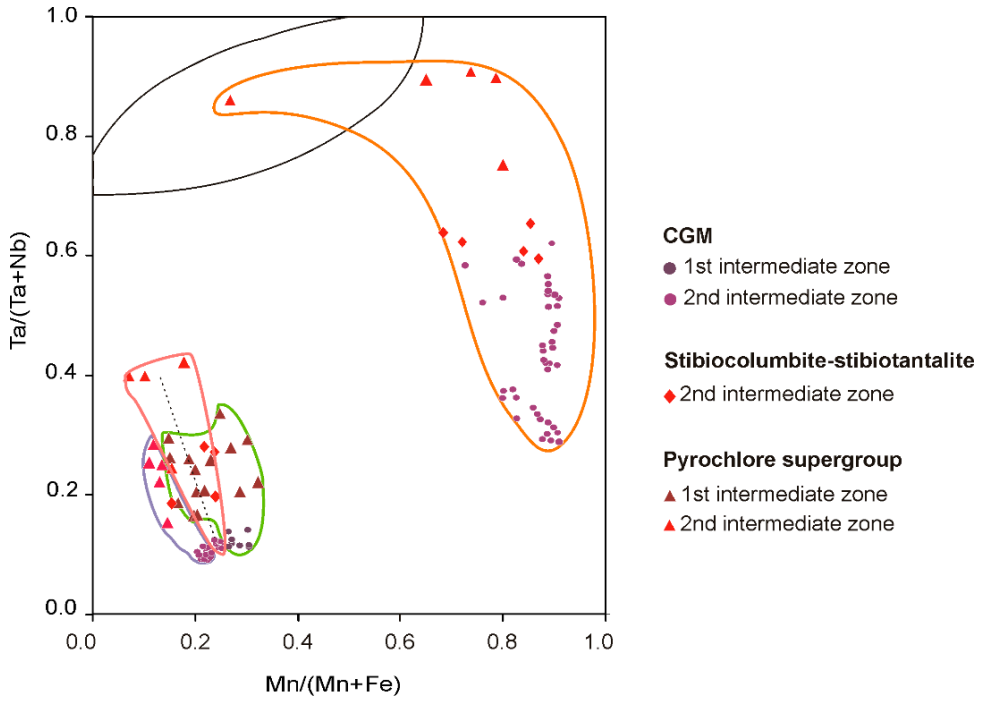

Figure 24. Composition of CGM, pyrochlore supergroup, stibiocolumbite and stibiotantalite of selected crystals of type-IV pegmatites from Giraúl plotted in the CGM quadrilateral.

The high fugacity of fluorine in this type of pegmatite, evidenced by the high F content in some phosphates and silicates, can be expected to modify the mineralogy of Nb-Ta oxides in favour of microlite [68,71,72]. Fluorine has been considered to carry out an important role in the fractionation of Nb-Ta minerals, as this element increases the solubility of Nb and Ta [73,74]. However, other experimental studies have shown that F has a limited control, being more important the temperature and the aluminium saturation in the precipitation of the CGM [75]. In cases where fluorine is scarce, columbite-(Fe) is mainly formed and evolves to tantalite-(Fe), ixiolite and ferrotapiolite. Examples are the pegmatites of Yellowknife, Northwest Territories, Canada [76], the pegmatites of Cap de Creus, Catalonia, Spain [31] and the pegmatites of Bastar-Malkangiri, India [77].

Members of the pyrochlore supergroup are the dominant Nb-Ta oxide minerals in the last stages of crystallisation of the most evolved pegmatites and replace the CGM minerals. Their occurrence could be due to cases with a high activity of F in the magma. The higher this activity, the higher will be the formation of fluoride complexes in the magma; in consequence, at least part of Ta and Nb do not precipitate in the magmatic stages but remain in the exsolved residual fluid. In addition, an increase in the alkalinity of this residual fluid would cause the crystallization as pyrochlore during postmagmatic sodic metasomatism. This mechanism has been proposed for the albitic apical granites of Kaffo, in the Ririwai complex, Nigeria, where pyrochlore is the main Nb-rich mineral and appears in the late stages of albitisation [78].

The increase in Ta with respect to Nb with the evolution is observed in granitic rocks not only on the scale of the Nb-Ta oxides but also in whole rock [18].

5.4. Comparison of the Nb-Ta Fractionation Trend with Other Pegmatite Fields

The trend of Ta enrichment in the field at Giraúl produces only moderate enrichments, as rarely do the compositions of the crystals plot in the compositional fields of tantalite-(Fe) or tantalite-(Mn). The few analyses that plot in these fields correspond to partial replacements of other larger crystals, much richer in Nb. This enrichment trend shows a low range when compared to the evolutionary trends of other classic pegmatites from the beryl-columbite-phosphate subtype, such as Cap de Creus (Catalonia), Yellowknife or Greer Lake (Canada). Columbite crystals of Giraúl are much richer in Mn, but less enriched in Ta (Figure 25). In all these fields, the trend is more complete. A Ta enrichment trend reflecting the evolution across the intermediate zones has been clearly observed in Giraúl only in type V pegmatites (Figure 18) and do not exhibits simultaneous enrichments in Ta and Mn, indicative of the higher evolution found in other strongly evolved pegmatites [79]. The simultaneous enrichment trends in Mn and Ta have also been explained by fractionation of these elements towards residual Li- and F- enriched magmas [72]; however, in Giraúl the highest enrichments are only observed in the crystals of stibiotantalite and in the strongly replaced crystals. Hence, these textural data are better explained by interaction of the exsolved hydrothermal fluids with the above-formed CGM crystals, rather than as a result of an evolved magmatic trend. In summary, this low evolved trend suggests that the Giraúl field only presents moderate enrichments in rare elements.

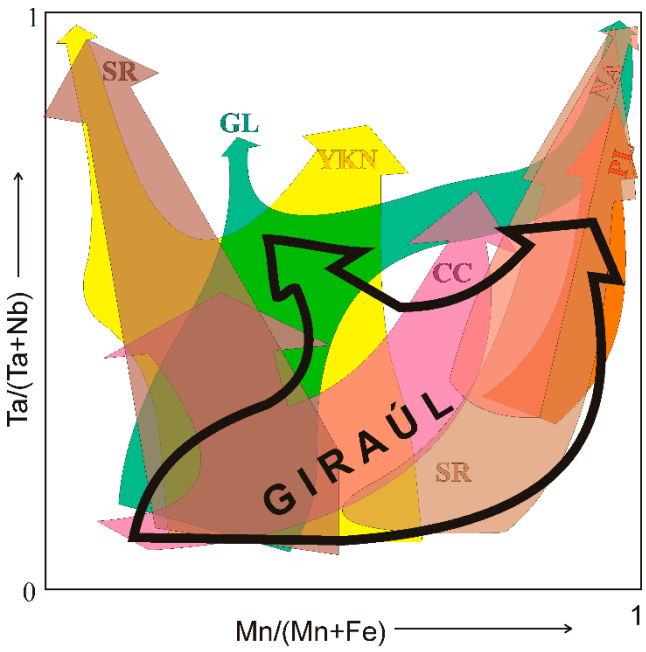

Figure 25. Comparison of the evolution trend of the chemical composition of CGM from the pegmatite field of Giraúl (thick line) with other evolved pegmatite fields. CC, Cap de Creus [31]; SR, Separation Rapids pluton [68]; PL, Pakeagama Lake [80]; YKN, Yellowknife [77]; NA, North Aubry [81]; GL, Greer Lake [72].

5.5. Mechanisms of Concentration of Nb and Ta

The increase in the ratio Ta/(Ta + Nb) with the evolution, observed in the pegmatites of Giraúl and in most of the pegmatite fields, is attributed to a higher solubility of the final member tantalite compared to that of columbite in the pegmatite melt [14,82]. The final columbite-(Fe) member is an order of magnitude more soluble than that of columbite-(Mn) [83]. The variation in the ratio Mn/(Mn + Fe) normally also increases with fractionation. However, this ratio shows a weak increase with the evolution

in the Giraúl pegmatites. This can be explained because this ratio depends fundamentally on the relationship of these minerals and others that contain Fe and Mn that coexist with them [62–83]. There is currently a strong controversy over the transport mechanism of rare elements, and in particular, of Zr, Hf, Nb and Ta. The most accepted hypothesis is that these elements are not mobile in hydrothermal systems, and that their concentration occurs exclusively during magmatic episodes [15,84]. However, in the last episodes of magmatic crystallisation, the unmixing process between a fluid phase and the melt has been recorded in fluid inclusion studies [85–87]. In this hydrothermal-magmatic transition a deuteric silicate liquid was described as a transitional phase between a magma and an aqueous fluid [88]. The hydrogen isotopic composition of micas from the Varuträsk rare-element pegmatite was also used as an argument to the occurrence of mica-rich metasomatic replacements by an aqueous fluid exsolved from the magma [89].

According to experimental studies, during this separation Nb and Ta are partitioned into the magma [11,15,90]. However, according to [91], magmatic fractionation alone cannot explain the formation of leucogranites with high Ta/(Ta + Nb) ratios. Instead, they propose that these values can be explained by the fractional crystallisation together with a subsolidus hydrothermal remobilisation.

Some Ta-rich minerals, particularly minerals of the pyrochlore supergroup, crystallised in late cavities. In the case of the most evolved and Ta-rich pegmatites of Giraúl, columbite is often partly replaced by Ta-rich phases. These replacements could perhaps occur partly by diffusion in the solid state, but without any doubt they are produced at least in Giraúl as fracture fillings, in which microlite tend to form idiomorphic crystals. The mineral association found in these replacements suggests that they have formed at the latest stages of crystallisation of pegmatite, in association with muscovite. All this shows that these elements can be transported or, at least, remobilised, by the late hydrothermal fluids.

Other argument that supports that Ta can be transported by exsolved fluids is the occurrence of high Ta contents in metasomatised host rocks of the Cape Cross–Uis pegmatite belt, Namibia [92].

In addition, the composition of the pyrochlore supergroup in the Giraúl pegmatites has a wide range, with a Ta/(Ta + Nb) values higher than that of the hosting minerals of the CGM where they are hosted. This increase in the Ta/(Ta + Nb) values was also found in other pegmatite fields [93,94]. This fact and the richness in U, Sb, Pb, Ca, Sr suggest that these minerals have been formed from the reaction of a hydrothermal fluid rich in these elements with the previous Nb-Ta minerals. This fluid likely leaves the pegmatite body in convection-driven cells, interacts with the country rocks, and re-enters the pegmatite [95]. This enrichment in Ta suggests that not only Ta but also minor Nb were transported in the hydrothermal fluids. However, in other cases similar Ta/(Ta + Nb) values were observed between the minerals of the pyrochlore supergroup and their precursors [25,41], indicating that Nb and Ta show a very limited mobility in the hydrothermal alteration of these granitic pegmatites. However, in other cases, such as in the Giraúl pegmatites, these elements show a certain mobility. Niobium is considered immobile during these replacements, whereas Ta, Y, U, and Zr can be mobilised during the late hydrothermal fluids exsolved from pegmatite-forming melts [96].

What kind of fluids are able to carry these metals? The answer lies in the composition of the late-forming minerals of the pegmatite, in particular, those of the series montebrasite-amblygonite, micas and tourmaline group. All these minerals are formed in several stages of the crystallisation of the pegmatite, but all of them have in common that in the first stages (crystallisation of the intermediate zones) they are poor in F, whereas the crystals that have formed during the late processes (notably, the quartz-muscovite-elbaite veins) are highly enriched in F, indicating a high activity of F in the later fluids. The presence of large amounts of phosphorus and lithium in the magma plays a determining role in the pegmatite petrogenesis, since it further reduces the liquidus temperature [97]. Therefore, these results point to an enrichment in F in the later stages of crystallisation, which facilitates the transport of Ta. Other highly incompatible elements of the HFSE type such as Sn, Sb, U, and in part Pb and Bi are present in this association. These elements usually indicate a high degree of fractionation [25].

6. Conclusions

Hafnon shows a clear but moderate enrichment trend in zircon, from the less evolved pegmatites towards the most evolved pegmatites; moreover, there is an increase in the ratios Hf/(Zr + Hf) from every pegmatite as the crystallisation process becomes more advanced. An identical behavior at the scales of field and pegmatite, but also crystal, is observed in the Ta/(Ta + Mn) values. The Nb-Ta crystals of the Giraúl pegmatites follow an evolutionary trend represented by variations in the Ta/(Ta + Nb) ratio, whereas the variation in the Mn/(Mn + Fe) ratio is limited. This evolution is attributed to a higher solubility of the tantalite end-member respect to columbite in the evolved pegmatite-forming melts, at the field scale, and to remobilisation by hydrothermal exsolved fluids, at the scale of body, at least in the late episodes.

The Mn/(Mn + Fe) value increases markedly during the late stages of replacement in type-IV pegmatites. Variation in this ratio depends on the other (Fe, Mn)-bearing minerals that coexist with these minerals. Oscillatory zoning, present in most of columbite-group crystals, indicates a growth under disequilibrium conditions. Crystals with convoluted patterns formed by metasomatic processes. Stibiocolumbite, bismutocolumbite and members of the pyrochlore supergroup, as well as other Ta-rich minerals as tapiolite also formed as late minerals such as indicated by their location in veins. They formed from the reaction of hydrothermal fluids with previous Nb-Ta oxide minerals.

Pyrochlore-supergroup minerals exhibit a wide compositional variation. The Nb-Ta content is similar to that of neighbouring CGM in U-dominant pyrochlore but it is higher in Pb and Sb-dominant pyrochlore. This fact and the richness in U, Sb, Pb, Ca, Sr indicate the metasomatic origin of these minerals. Thus, pyrochlore-supergroup minerals formed from the reaction of hydrothermal fluids with the pre-existing Nb-Ta oxides. Nevertheless, the Ta enrichment suggests that Nb and Ta were transported in the hydrothermal fluids.

As a whole, the relatively low enrichment of Hf in zircon and the moderate enrichments of Mn and Ta n the most evolved pegmatites suggest that the Giraúl field has only a moderate potential as resource for critical elements.

Author Contributions: Fieldwork, A.O.G., J.-C.M., E.A.M., A.B.N.; acquisition of analytical data: A.O.G., J.-C.M.; P.A., interpretation: A.O.G., J.-C.M., P.A., A.P.; writing. P.A.; review, S.A., A.C. and all the authors.

Funding: This study benefitted from the budged granted by the Generalitat de Catalunya (Autonomous Government of Catalonia) to the Consolidated Research Group SGR 444.

Acknowledgments: The Departament of Geology of the Agostinho Neto University from Luanda (Angola) provided all the necessary logistic support for the field study. A.O.G. benefit with a doctoral grant to carry out the study.

Conflicts of Interest: The authors declare no conflict of interest. The funders had no role in the design of the study; in the collection, analyses, or interpretation of data; in the writing of the manuscript, or in the decision to publish the results.

References

1. Linnen, R.L. Granitic Pegmatites as Sources of Strategic Metals. *Elements* **2012**, *8*, 275–280. [CrossRef]
2. London, D. Pegmatites. *Can. Mineral.* **2008**, *10*, 347.
3. Mackay, A.R.; Simandl, G.J. Geology, market and supply chain of niobium and tantalum—A review. *Mineral. Depos.* **2014**, *49*, 1025–1047. [CrossRef]
4. Nikishina, E.E.; Drobot, D.V.; Lebedeva, E.N. Niobium and tantalum: State of the world market, application fields, and sources of raw materials. Part 2. *Russ. J. Non-Ferr. Met.* **2014**, *55*, 130–140. [CrossRef]
5. Černý, P.; Meintzer, R.E.; Anderson, A.J. Extreme fractionation in rare-element granitic pegmatites: Selected examples of data and mechanisms. *Can. Mineral.* **1985**, *23*, 381–421.
6. Mulja, T.; Williams-Jones, A.E.; Martin, R.F.; Wood, S.A. Compositional variation and structural state of columbite-tantalite in rare-element granitic pegmatites of the Preissac-Lacorne batholith, Quebec, Canada. *Am. Mineral.* **1996**, *81*, 146–157. [CrossRef]

7. Ercit, T.S. REE-enriched granitic pegmatites. In *Rare-Element Geochemistry and Ore Deposits: Geological Association of Canada Short Course Notes*; Linnen, R.L., Samson, I.M., Eds.; Mineralogical Association of Canada: Québec, QC, Canada, 2005; Volume 17, pp. 257–296.
8. Raimbault, L.; Burnol, L. The Richemont rhyolite dyke, Massif Central, France; a subvolcanic equivalent of rare-metal granites. *Can. Mineral.* **1998**, *36*, 265–282.
9. Stepanov, A.; Mavrogenes, J.A.; Meffre, S.; Davidson, P. The key role of mica during igneous concentration of tantalum. *Contrib. Mineral. Petrol.* **2014**, *167*, 1009. [CrossRef]
10. Škoda, R.; Novák, M. Y, REE, Nb, Ta, Ti-oxide (AB_2O_6) minerals from REL–REE euxenite-subtype pegmatites of the Třebíč Pluton, Czech Republic; substitutions and fractionation trends. *Lithos* **2007**, *95*, 43–57. [CrossRef]
11. Kaeter, D.; Barros, R.; Menuge, J.F.; Chew, D.M. The magmatic–hydrothermal transition in rare-element pegmatites from southeast Ireland: LA-ICP-MS chemical mapping of muscovite and columbite–tantalite. *Geochim. Cosmochim. Acta* **2018**, *240*, 98–130. [CrossRef]
12. Deetman, S.; van Oers, L.; van der Voet, E.; Tukker, A. Deriving European tantalum flows using trade and production statistics. *J. Ind. Ecol.* **2018**, *22*, 166–179. [CrossRef]
13. Anderson, M.O.; Lentz, D.R.; McFarlane, M.; Falck, H. A geological, geochemical and textural study of a LCT pegmatite: Implications for the magmatic versus metasomatic origin of Nb–Ta mineralization in the Moose II pegmatite, Northwest Territories. *J. Geosci.* **2013**, *58*, 299–320. [CrossRef]
14. Linnen, R.L.; Keppler, H. Columbite solubility in granitic melts: Consequences for the enrichment and fractionation of Nb and Ta in the Earth's crust. *Contrib. Mineral. Petrol.* **1997**, *128*, 213–227. [CrossRef]
15. Linnen, R.L. The solubility of Nb-Ta-Zr-Hf-W in granitic melts with Li and Li + F: Constraints for mineralization in rare metal granites and pegmatites. *Econ. Geol.* **1998**, *93*, 1013–1025. [CrossRef]
16. Belkasmi, M.; Cuney, M.; Pollard, P.J.; Bastoul, A. Chemistry of the Ta-Nb-Sn-W oxide minerals from the Yichun rare metal granite (SE China): Genetic implications and comparison with Moroccan and French Hercynian examples. *Mineral. Mag.* **2000**, *64*, 507–523. [CrossRef]
17. Akoh, J.U.; Ogunleye, P.O.; Ibrahim, A.A. Geochemical evolution of micas and Sn-, Nb-, Ta-mineralization associated with the rare metal pegmatite in Angwan Doka, central Nigeria. *J. Afr. Earth Sci.* **2015**, *112*, 24–36. [CrossRef]
18. Dostal, J.; Chaterjee, A.K. Contrasting behaviour of Nb/Ta and Zr/Hf ratios in a peraluminous granitic pluton (Nova Scotia, Canada). *Chem. Geol.* **2000**, *163*, 207–218. [CrossRef]
19. Neiva, A.M.R.; Gomes, M.E.P.; Silva, P.B. Two generations of zoned crystals of columbite-group minerals from granitic aplite–pegmatite in the Gouveia area, central Portugal. *Eur. J. Mineral.* **2015**, *27*, 771–782. [CrossRef]
20. Zhu, Z.Y.; Wang, R.C.; Che, X.D.; Zhu, J.C.; Wei, X.L.; Huang, X. Magmatic–hydrothermal rare-element mineralization in the Songshugang granite (northeastern Jiangxi, China): Insights from an electron-microprobe study of Nb–Ta–Zr minerals. *Ore Geol. Rev.* **2015**, *65*, 749–760. [CrossRef]
21. Alfonso, P.; Hamid, S.A.; García-Vallès, M.; Llorens, T.; Moro, F.L.; Tomasa, O.; Calvo, D.; Oliva, J.; Parcerisa, D.; García-Polonio, F. Textural and mineral-chemistry constraints on columbite-group minerals in the Penouta deposit: Evidence from magmatic and fluid-related processes. *Mineral. Mag.* **2018**, *82*, S199–S222. [CrossRef]
22. Soares de Carvalho, G. Geologia do Deserto de Moçâmedes (Angola). *Mem. Junta Investig. Ultramar* **1961**, *26*, 227.
23. Černý, P.; Ercit, T.S. The classification of granitic pegmatites revisited. *Can. Mineral.* **2005**, *43*, 2005–2026. [CrossRef]
24. Černý, P. (Ed.) Anatomy and classification of granitic pegmatites. In *Granitic Pegmatites in Science and Industry*; Short Course Handbook; Mineralogical Association of Canada: Québec, QC, Canada, 1982; Volume 8, pp. 1–39.
25. Černý, P.; Chapman, R.; Ferreira, K.; Smeds, S.A. Geochemistry of oxide minerals of Nb, Ta, Sn, and Sb in the Varuträsk granitic pegmatite, Sweden: The case of an "anomalous" columbite-tantalite trend. *Am. Mineral.* **2004**, *89*, 505–518. [CrossRef]
26. Goreva, J.S.; Ma, C.; Rossman, G.R. Fibrous nanoinclusions in massive rose quartz: The origin of rose coloration. *Am. Mineral.* **2001**, *86*, 466–472. [CrossRef]
27. Larsen, R.B.; Henderson, I.; Ihlen, P.M.; Jacamon, F. Distribution and petrogenetic behaviour of trace elements in granitic pegmatite quartz from South Norway. *Contrib. Mineral. Petrol.* **2004**, *147*, 615–628. [CrossRef]

28. Ma, C.; Goreva, J.S.; Rossmann, G.R. Fibrous nano-inclusions in massive rose quartz: HRTEM and AEM investigations. *Am. Mineral.* **2002**, *87*, 269–276. [CrossRef]
29. Keller, P. The occurrence of Li-Fe-Mn phosphate minerals in granitic pegmatites of Namibia. *Commun. Geol. Surv. Namib.* **1991**, *7*, 21–34.
30. Roda, E.; Pesquera, A.; Fontan, F.; Keller, P. Phosphate mineral associations in the Canada pegmatite (Salamanca, Spain): Paragenetic relationships, chemical compositions, and implications for pegmatite evolution. *Am. Mineral.* **2004**, *89*, 110–125. [CrossRef]
31. Alfonso, P.; Corbella, M.; Melgarejo, J.C. Nb-Ta- minerals from the Cap de Creus pegmatite Field, eastern Pyrenees: Distribution and geochemical trends. *Mineral. Petrol.* **1995**, *55*, 53–69. [CrossRef]
32. Simmons, W.B.S.; Webber, K.L. Pegmatite genesis: State of the art. *Eur. J. Mineral.* **2008**, *20*, 421–438. [CrossRef]
33. Quensel, P. Minerals of the Varuträsk pegmatite. I: The lithium manganese phosphates. *Geol. Fören. Förhandl.* **1937**, *59*, 77–96. [CrossRef]
34. Mason, B. Minerals of the Varuträsk pegmatite. XXIII. Some ironmanganese phosphate minerals and their alteration products, with special reference to material from Varuträsk. *Geol. Fören Förhandl.* **1941**, *63*, 117–165. [CrossRef]
35. Fransolet, A.M.; Keller, P.; Fontan, F. The phosphate mineral associations of the Tsaobismund pegmatite, Namibia. *Contrib. Mineral. Petrol.* **1986**, *92*, 502–517. [CrossRef]
36. Malló, A.; Fontan, F.; Melgarejo, J.C.; Mata, J.M. The Albera zoned pegmatite field, eastern Pyrenees, France. *Mineral. Petrol.* **1995**, *55*, 103–116. [CrossRef]
37. Baijot, M.; Hatert, F.; Dal Bo, F.; Philippo, S. Mineralogy and petrography of phosphate mineral associations from the Jocão pegmatite, Minas Gerais, Brazil. *Can. Mineral.* **2014**, *52*, 373–397. [CrossRef]
38. Sebastian, A.; Lagache, M. Experimental study of lithium-rich granitic pegmatites; Part I, Petalite + albite + quartz equilibrium. *Am. Mineral.* **1991**, *76*, 205–210.
39. Thomas, R.J.; Bühmann, D.; Bullen, W.D.; Scogings, A.J.; De Bruin, D. Unusual spodumene pegmatites from the late Kibaran of southern Natal, South Africa. *Ore Geol. Rev.* **1994**, *9*, 161–182. [CrossRef]
40. Stilling, A.; Černý, P.; Vanstone, P.J. The Tanco Pegmatite at Bernic Lake, Manitoba; XVI, Zonal and bulk compositions and their petrogenetic significance. *Can. Mineral.* **2006**, *44*, 599–623. [CrossRef]
41. Selway, J.B.; Breaks, F.W.; Tindle, A.G. A review of rare-element (Li-Cs-Ta) pegmatite exploration techniques for the Superior Province, Canada, and large worldwide tantalum deposits. *Explor. Min. Geol.* **2005**, *14*, 1–30. [CrossRef]
42. Demartis, M.; Melgarejo, J.C.; Colombo, F.; Alfonso, P.; Coniglio, J.E.; Pinotti, L.P.; D'Eramo, F.J. Extreme F activities in late pegmatitic events as a key factor for LILE and HFSE enrichment: The Ángel pegmatite, central Argentina. *Can. Mineral.* **2014**, *52*, 247–269. [CrossRef]
43. Peretyazhko, I.S.; Zagorsky, V.Y.; Smirnov, S.Z.; Mikhailov, M.Y. Conditions of pocket formation in the Oktyabrskaya tourmaline-rich gem pegmatite (the Malkhan field, Central Transbaikalia, Russia). *Chem. Geol.* **2004**, *210*, 91–111. [CrossRef]
44. Novák, M.; Černý, P.; Cempirek, J.; Srein, V.; Filip, J. Ferrotapiolite as a pseudomorph of stibiotantalite from the Lăstovičky lepidolite pegmatite, czech republic; an example of hydrothermal alteration at constant Ta/(Ta + Nb). *Can. Mineral.* **2004**, *42*, 1117–1128. [CrossRef]
45. Atencio, D.; Andrade, M.B.; Christy, A.G.; Gieré, R.; Kartashov, P.M. The pyrochlore supergroup of minerals nomenclature. *Can. Mineral.* **2010**, *48*, 673–698. [CrossRef]
46. Chukanov, N.V.; Kuzmina, O.V.; Zadov, A.E. Bismutopyrochlore $(Bi,U,Ca,Pb)_{1+x}(Nb,Ta)_2O_6(OH)\cdot nH_2O$—A new mineral from the pegmatites of the Mika vein (eastern Pamirs). *Zap. Vsesoyuznoye Mineral. Obs.* **1999**, *128*, 36–41. (In Russian)
47. Lumpkin, G.R.; Ewing, R.C.; Williams, C.T.; Mariano, A.N. An overview of the crystal chemistry, durability, and radiation damage effects of natural pyrochlore. *MRS Online Proc. Libr. Arch.* **2000**, *663*, 921. [CrossRef]
48. Matyszczak, W. Liandratite from Karkonosze pegmatites, Sudetes, Southwestern Poland. *Mineral. Petrol.* **2018**, *112*, 357–370. [CrossRef]
49. Černý, P.; Novák, M.; Chapman, R.; Ferreira, K.J. Subsolidus behavior of niobian rutile from the Písek region, Czech Republic: A model for exsolution in W-and Fe^{2+} >> Fe^{3+}-rich phases. *J. Geosci.* **2007**, *52*, 143–159. [CrossRef]

50. Neiva, A.M.R. Geochemistry of cassiterite and its inclusions and exsolution products from tin and tungsten deposits in Portugal. *Can. Mineral.* **1996**, *34*, 745–768.
51. Černý, P. Rare-element granitic pegmatites, part 1. Anatomy and internal evolution of pegmatite deposits. *Geosci. Can.* **1991**, *18*, 49–67.
52. Černý, P.; Roberts, W.L.; Ercit, T.S.; Chapman, R. Zirconium and hafnium in minerals of the columbite and wodginite groups from granitic pegmatites. *Can. Mineral.* **1985**, *45*, 185–202. [CrossRef]
53. Correia Neves, J.C.; Nunes, J.L.; Sahama, T.G. High hafnium members of the zircon-hafnon series from the granite pegmatites of Zambézia, Mozambique. *Contrib. Mineral. Petrol.* **1974**, *48*, 73–80. [CrossRef]
54. Yin, R.; Wang, R.C.; Zhang, A.C.; Hu, H.; Zhu, J.C.; Rao, C.; Zhang, H. Extreme fractionation from zircon to hafnon in the Koktokay No. 1 granitic pegmatite, Altai, northwestern China. *Am. Mineral.* **2013**, *98*, 1714–1724. [CrossRef]
55. Kudryashov, N.M.; Skublov, S.G.; Galankina, O.L.; Udoratina, O.V.; Voloshin, A.V. Abnormally high-hafnium zircon from rare-metal pegmatites of the Vasin-Mylk deposit (the northeastern part of the Kola Peninsula). *Geochemistry* **2019**, *2019*. [CrossRef]
56. Fontan, F.; Monchoux, P.; Autefage, F. Présence de zircons hafnifères dans des pegmatites granitiques des Pyrénées ariégeoises; leur relation avec les niobotantalates. *Bull. Mineral.* **1980**, *103*, 88–91.
57. Wang, R.C.; Fontan, F.; Xu, S.J.; Chen, X.M.; Monchoux, P. Hafnian zircon from the apical part of the Suzhou granite, China. *Can. Mineral.* **1996**, *34*, 1001–1010.
58. Zaraisky, G.P.; Aksyuk, A.M.; Devyatova, V.N.; Udoratina, O.V.; Chevychelov, V.Y. The Zr/Hf ratio as a fractionation indicator of rare-metal granites. *Petrology* **2009**, *17*, 25. [CrossRef]
59. Van Lichtervelde, M.; Holtz, F.; Hanchar, J.M. Solubility of manganotantalite, zircon and hafnon in highly fluxed peralkaline to peraluminous pegmatitic melts. *Contrib. Mineral. Petrol.* **2010**, *160*, 17–32. [CrossRef]
60. Barsanov, G.P.; Yeremin, N.I.; Sergeyeva, N.Y.E. Columbite-tantalite zoning as revealed by electron-probe microanalysis. *Dokl. Akad. Nauk SSSR* **1971**, *201*, 174–176. (In Russian)
61. Černý, P.; Ercit, T.S.; Wise, M.A. The tantalite-tapiolite gap: Natural assemblages versus experimental data. *Can. Mineral.* **1992**, *30*, 587–596.
62. Novák, M.; Chládek, Š.; Uher, P.; Gadas, P. Complex magmatic and subsolidus compositional trends of columbite-tantalite in the beryl-columbite Sejby granitic pegmatite, Czech Republic: Role of crystal-structural constraints and associated minerals. *J. Geosci.* **2018**, *63*, 253–263. [CrossRef]
63. Lahti, S.I. Zoning in columbite-tantalite crystals from the granitic pegmatites of the Erajarvi area, southern Finland. *Geochim. Cosmochim. Acta* **1987**, *51*, 509–517. [CrossRef]
64. Putnis, A.; Fernaández-Diaz, L.; Prieto, M. Experimentally produced oscillatory zoning in the (Ba,Sr)SO_4 solid solution. *Nature* **1992**, *358*, 743–745. [CrossRef]
65. Černý, P. Geochemical and petrogenitic features of mineralisation in rare-element granitic pegmatites in the light of current research. *Appl. Geochem.* **1992**, *7*, 393–416.
66. Putnis, A. Mineral replacement reactions: From macroscopic observations to microscopic mechanisms. *Mineral. Mag.* **2002**, *66*, 689–708. [CrossRef]
67. Černý, P.; Novák, M.; Chapman, R. Effects of sillimanite-grade metamorphism and shearing on Nb-Ta oxide minerals in granitic pegmatites: Marsikov, Northern Moravia, Czechoslovakia. *Can. Mineral.* **1992**, *30*, 699–718.
68. Tindle, A.G.; Breaks, F.W. Oxide minerals of the Separation Rapids rare-element granitic pegmatite group, Northwestern Ontario. *Can. Mineral.* **2000**, *36*, 609–635.
69. Tindle, A.G.; Breaks, F.W.; Webb, P.C. Wodginite-group minerals from the Separation Rapids rare-element granitic pegmatite group, Northwestern Ontario. *Can. Mineral.* **1998**, *36*, 637–658.
70. Černý, P.; Ercit, T.S. Some recent advances in the mineralogy and geochemistry of Nb and Ta in rare-element granitic pegmatites. *Bull. Mineral.* **1985**, *108*, 499–532. [CrossRef]
71. Černý, P. Characteristics of pegmatite deposits of tantalum. In *Lanthanides, Tantalum and Niobium*; Möller, P., Černý, P., Saupe, F., Eds.; Springer: Berlin/Heidelberg, Germany; New York, NY, USA, 1989; pp. 139–195.
72. Černý, P.; Goad, B.E.; Hawthorne, F.C.; Chapman, R. Fractionation trends of the Nb- and Ta- bearing oxide minerals in the Greer Lake pegmatitic granite and its pegmatite aureole, southeastern Manitoba. *Am. Mineral.* **1986**, *71*, 501–517.
73. Keppler, H. Infuence of fuorine on the enrichment of high field strength trace elements in granitic rocks. *Contrib. Mineral. Petrol.* **1993**, *114*, 479–488. [CrossRef]

74. Zaraisky, G.P.; Korzhinskaya, V.; Kotova, N. Experimental studies of Ta_2O_5 and columbite–tantalite solubility in fluoride solutions from 300 to 550 C and 50 to 100 MPa. *Miner. Petrol.* **2010**, *99*, 287–300. [CrossRef]
75. Aseri, A.A.; Linnen, R.L.; Che, X.D.; Thibault, Y.; Holtz, F. Effects of fluorine on the solubilities of Nb, Ta, Zr and Hf minerals in highly fluxed water-saturated haplogranitic melts. *Ore Geol. Rev.* **2015**, *64*, 736–746. [CrossRef]
76. Wise, M.A.; Meintzer, R.E.; Černý, P. The Yellowknife pegmatite Field: Mineralogy and geochemistry of Nb-Ta-Sn oxide minerals. *Contrib. Geol. NWT* **1986**, *2*, 15–25.
77. Pal, D.C.; Biswajit, M.; Bernhardt, H.J. Contrasting fluid inclusion characteristics of staniferous and non-staniferous pegmatites of Southeast Bastar, Central India. *Ore Geol. Rev.* **2007**, *30*, 30–35. [CrossRef]
78. Ogunleye, P.O.; Garba, I.; Ike, E.C. Factors contributing to enrichment and crystallization of niobium in pyrochlore in the Kaffo albite arfvedsonite granite, Ririwai Complex, Younger Granites province of Nigeria. *J. Afr. Earth Sci.* **2006**, *44*, 372–382. [CrossRef]
79. Tadesse, S.; Zerihun, D. Composition, fractionation trend and zoning accretion of the columbite-tantalite group of minerals in the Kenticha rare-metal field (Adola, southern Ethiopia). *J. Afr. Earth Sci.* **1996**, *23*, 411–431. [CrossRef]
80. Smith, S.R.; Foster, G.L.; Romer, R.L.; Tindle, A.G.; Kelley, S.P.; Noble, S.R.; Horstwood, M.; Breaks, F.W. U-Pb columbite-tantalite chronology of rare-element pegmatites using TIMS and Laser Ablation-Multi Collector-ICP-MS. *Contrib. Mineral. Petrol.* **2004**, *147*, 549–564. [CrossRef]
81. Breaks, F.W.; Selway, J.B.; Tindle, A.G. *Fertile Peraluminous Granites and Related Rare Element Mineralization in Pegmatites, Superior Province, Northwest and Northeast Ontario: Operation Treasure Hunt*; Open File Report 6099; Ontario Geological Survey: Sudbury, ON, Canada, 2003; 179p.
82. Timofeev, A.; Migdisov, A.A.; Williams-Jones, A.E. An experimental study of the solubility and speciation of tantalum in fluoride-bearing aqueous solutions at elevated temperature. *Geochim. Cosmochim. Acta* **2017**, *197*, 294–304. [CrossRef]
83. Linnen, R.L. Ferrocolumbite-manganotantalite trends in granites and pegmatites: Experimental and natural constraints. *Geol. Soc. Amer. Abstr. Prog.* **2004**, *36*, 115.
84. Linnen, R.L.; Samson, I.M.; Williams-Jones, A.E.; Chakhmouradian, A.R. Geochemistry of the Rare-Earth Element, Nb, Ta, Hf, and Zr Deposits. In *Treatise on Geochemistry*, 2nd ed.; Holland, H.D., Turekian, K.K., Eds.; Elsevier: Oxford, UK, 2014; pp. 543–564.
85. Kamenetsky, V.S.; Naumov, V.B.; Davidson, P.; van Achterbergh, E.; Ryan, C.G. Immiscibility between silicate magmas and aqueous fluids: A melt inclusion pursuit into the magmatic-hydrothermal transition in the Omsukchan Granite (NE Russia). *Chem. Geol.* **2004**, *210*, 73–90. [CrossRef]
86. Alfonso, P.; Melgarejo, J.C. Fluid evolution in the zoned rare-element pegmatite field at Cap de Creus, Catalonia, Spain. *Can. Mineral.* **2008**, *46*, 597–617. [CrossRef]
87. Mulja, T.; Williams-Jones, A.E. The physical and chemical evolution of fluids in rare-element granitic pegmatites associated with the Lacorne pluton, Québec, Canada. *Chem. Geol.* **2018**, *493*, 281–297. [CrossRef]
88. Wu, M.; Samson, I.M.; Zhang, D. Textural Features and Chemical Evolution in Ta-Nb Oxides: Implications for Deuteric Rare-Metal Mineralization in the Yichun Granite-Marginal Pegmatite, Southeastern China. *Econ. Geol.* **2018**, *113*, 937–960. [CrossRef]
89. Siegel, K.; Wagner, T.; Trumbull, R.B.; Jonsson, E.; Matalin, G.; Wälle, M.; Heinrich, C.A. Stable isotope (B, H, O) and mineral-chemistry constraints on the magmatic to hydrothermal evolution of the Varuträsk rare-element pegmatite (Northern Sweden). *Chem. Geol.* **2016**, *421*, 1–16. [CrossRef]
90. Tang, Y.; Zhang, H. Lanthanide tetrads in normalized rare element patterns of zircon from the Koktokay No. 3 granitic pegmatite, Altay, NW China. *Am. Mineral.* **2015**, *100*, 2630–2636. [CrossRef]
91. Ballouard, C.; Poujol, M.; Boulvais, P.; Branquet, Y.; Tartèse, R.; Vigneresse, J.L. Nb-Ta fractionation in peraluminous granites: A marker of the magmatic-hydrothermal transition. *Geology* **2016**, *44*, 231–234. [CrossRef]
92. Fuchsloch, W.C.; Nex, P.A.; Kinnaird, J.A. The geochemical evolution of Nb–Ta–Sn oxides from pegmatites of the Cape Cross–Uis pegmatite belt, Namibia. *Mineral. Mag.* **2019**, *83*, 161–179. [CrossRef]
93. Baldwin, J.R. Replacement phenomena in tantalum minerals from rare-metal pegmatites in South Africa and Namibia. *Mineral. Mag.* **1989**, *53*, 571–581. [CrossRef]
94. Uher, P.; Černý, P.; Chapman, R.; Határ, F.; Miko, O. Evolution of Nb,Ta-oxide minerals in the Prăsivá granitic pegmatites, Slovakia. II. External hydrothermal Pb,Sb overprint. *Can. Mineral.* **1998**, *36*, 535–545.

95. Martin, R.F.; De Vito, C. The late-stage miniflood of Ca in granitic pegmatites: An open-system acid-reflux model involving plagioclase in the exocontact. *Can. Mineral.* **2014**, *52*, 165–181. [CrossRef]
96. Duran, C.J.; Seydoux-Guillaume, A.M.; Bingen, B.; Gouy, S.; De Parseval, P.; Ingrin, J.; Guillaume, D. Fluid-mediated alteration of (Y, REE, U, Th)–(Nb, Ta, Ti) oxide minerals in granitic pegmatite from the Evje-Iveland district, southern Norway. *Mineral. Petrol.* **2016**, *110*, 581–599. [CrossRef]
97. Mysen, B.O.; Holtz, F.; Pichavant, M.; Beny, J.M.; Montel, J.M. The effect of temperature and bulk composition on the solution mechanism of phosphorus in peraluminous haplogranitic magma. *Am. Mineral.* **1999**, *84*, 1336–1345. [CrossRef]